iScience

CellPress
OPEN ACCESS

Article

Chronic lymphocytic leukemia B-cell-derived TNFα impairs bone marrow myelopoiesis

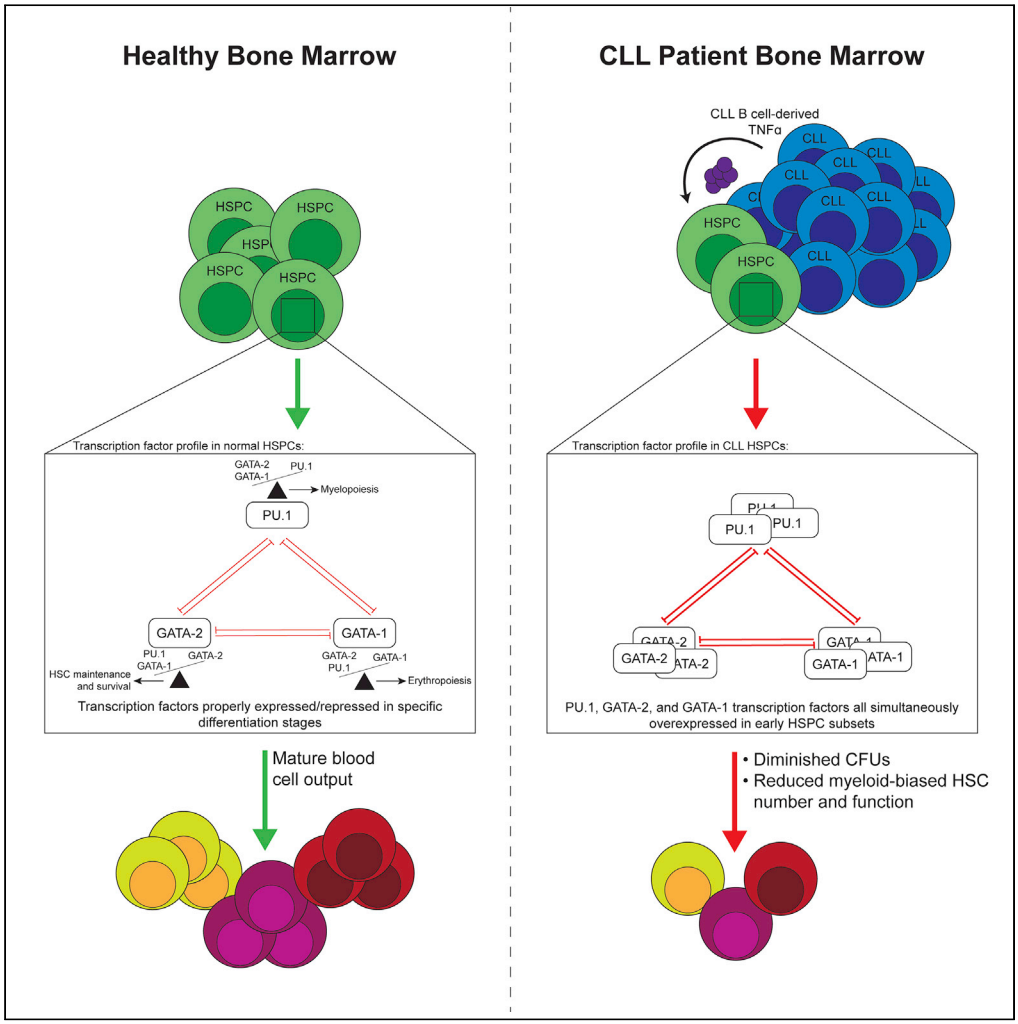

Bryce A. Manso, Jordan E. Krull, Kimberly A. Gwin, ..., Sameer A. Parikh, Neil E. Kay, Kay L. Medina

medina.kay@mayo.edu

Highlights

CLL patient BM HSPCs exhibit aberrant molecular and functional characteristics

CLL B-cell-derived TNFα upregulates PU.1 and GATA-2 in BM HSPCs

The effects of CLL B-cell-derived TNFα are reversible upon TNFα neutralization

Chronic TNFα exposure *in vitro* recapitulates *ex vivo* HSPC functional deficiencies

Manso et al., iScience *24*, 101994
January 22, 2021
https://doi.org/10.1016/j.isci.2020.101994

iScience

CellPress
OPEN ACCESS

Article

Chronic lymphocytic leukemia B-cell-derived TNFα impairs bone marrow myelopoiesis

Bryce A. Manso,[1,3] Jordan E. Krull,[1,2,3] Kimberly A. Gwin,[1] Petra K. Lothert,[1] Baustin M. Welch,[1,3] Anne J. Novak,[1,2] Sameer A. Parikh,[2] Neil E. Kay,[2] and Kay L. Medina[1,4,*]

Summary

TNFα is implicated in chronic lymphocytic leukemia (CLL) immunosuppression and disease progression. TNFα is constitutively produced by CLL B cells and is a negative regulator of bone marrow (BM) myelopoiesis. Here, we show that co-culture of CLL B cells with purified normal human hematopoietic stem and progenitor cells (HSPCs) directly altered protein levels of the myeloid and erythroid cell fate determinants PU.1 and GATA-2 at the single-cell level within transitional HSPC subsets, mimicking *ex vivo* expression patterns. Physical separation of CLL cells from control HSPCs or neutralizing TNFα abrogated upregulation of PU.1, yet restoration of GATA-2 required TNFα neutralization, suggesting both cell contact and soluble-factor-mediated regulation. We further show that CLL patient BM myeloid progenitors are diminished in frequency and function, an effect recapitulated by chronic exposure of control HSPCs to low-dose TNFα. These findings implicate CLL B-cell-derived TNFα in impaired BM myelopoiesis.

Introduction

Chronic lymphocytic leukemia (CLL), a chronic lymphoproliferative neoplasm characterized by accumulation of $CD19^+CD5^+$ B cells, is associated with global immunosuppression that clinically manifests as an inability to respond appropriately to immunologic challenges. As CLL B cells are widespread in the host, the immunosuppression may be directly induced by organ infiltrative accumulation of clonal leukemic cells or indirectly via leukemic cell-induced remodeling of tissue microenvironments (Forconi and Moss, 2015; Goldman, 2000; Kipps et al., 2017). In addition to accumulation in blood and secondary lymphoid organs, CLL B cells infiltrate the bone marrow (BM), the primary site of adult hematopoiesis. This latter feature is thus a threat to the normal and critical function of BM.

Steady-state BM hematopoiesis sustains blood cell genesis throughout life (immune cells, erythrocytes, and platelets) (Doulatov et al., 2012) and is a tightly regulated process (Novershtern et al., 2011). Importantly, BM hematopoiesis becomes myeloid-skewed with aging (Pang et al., 2017), a critical consideration as CLL is largely a disease of the aged. Aberrant hematopoiesis and BM dysfunction in CLL is understudied and historically suggested to most likely be an infiltrative remodeling that disrupts normal hematopoietic niches (Lagneaux et al., 1993). Reduced numbers of BM hematopoietic stem cells (HSCs) and their progeny may manifest due to competition with CLL B cells for hematopoietic niches, local increases in CLL-derived factors, or CLL-induced alterations in resident immune cells or components of the BM microenvironment (Fecteau and Kipps, 2012; Sala et al., 1998).

Given the chronic residence of CLL cells in BM, their likely competition with hematopoietic progenitors for essential niches, and the increased potential for leukemic and HSPC interactions, we hypothesized that BM hematopoietic capacity may be compromised in CLL patients. Indeed, our previous report confirmed significantly reduced frequencies of BM HSCs and their progeny in CLL patients compared with age-matched controls (Manso et al., 2019). In addition, we demonstrated hematopoietic functional impairment as evidenced by significantly reduced colony forming unit (CFU) capacity, revealing diminished production of myelo-erythroid progenitors. In this initial work we also showed that select BM hematopoietic progenitor subsets displayed aberrant transcription factor (TF) profiles at the protein level. Importantly, the collective features of impaired BM hematopoiesis in CLL patients were independent of the extent of BM infiltration by

[1]Department of Immunology, Mayo Clinic, 200 1st St SW, Rochester, MN 55905, USA

[2]Division of Hematology, Mayo Clinic, Rochester, MN 55905, USA

[3]Mayo Clinic Graduate School of Biomedical Sciences, Mayo Clinic, Rochester, MN 55905, USA

[4]Lead contact

*Correspondence: medina.kay@mayo.edu

https://doi.org/10.1016/j.isci.2020.101994

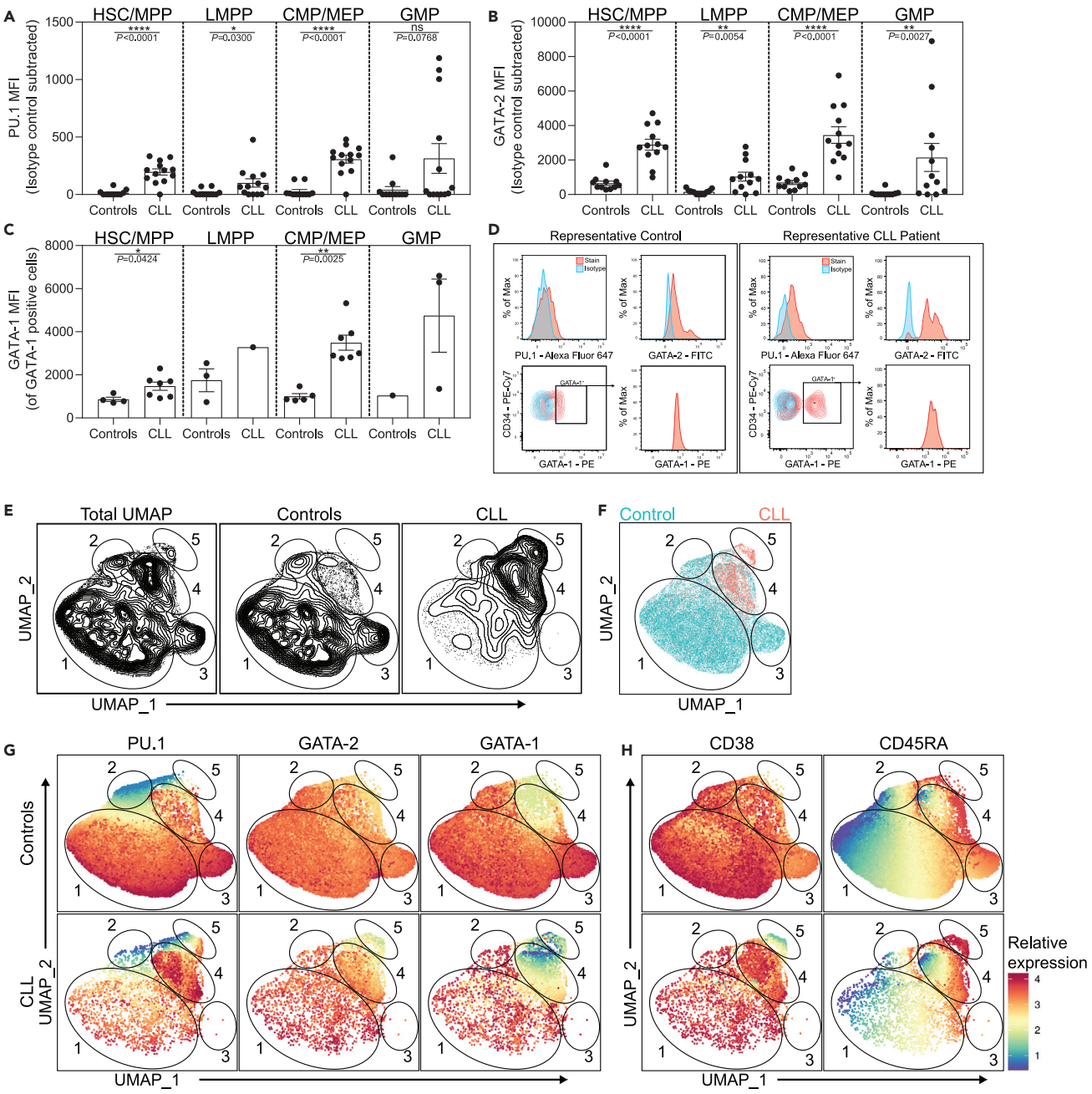

Figure 1. Altered expression of PU.1, GATA-2, and GATA-1 in CLL patient bone marrow progenitors

(A–C) Flow cytometry was performed on freshly isolated BM from controls and CLL patients to determine MFI (representative of protein levels) of (A) PU.1, (B) GATA-2, and (C) GATA-1 among HSPC progenitor subsets. Control n = 11 for PU.1, n = 11 for GATA-2, and n = 8 for GATA-1. CLL n = 13 for PU.1, n = 12 for GATA-2, and n = 7 for GATA-1. The displayed number of data points for GATA-1 are reduced due to several individuals containing no detectable GATA-1 protein. We were unable to perform statistical comparisons between control and CLL LMPPs and GMPs for GATA-1 MFI as few cells contained detectable GATA-1 protein: HSC/MPP ($Lin^-CD34^{hi}CD38^-CD45RA^-$), LMPP ($Lin^-CD34^{hi}CD38^-CD45RA^+$), CMP/MEP ($Lin^-CD34^+CD38^+CD45RA^-$), and GMP ($Lin^-CD34^+CD38^+CD45RA^+$). Data are presented as the mean ± SEM; individual points represent a unique donor and are representative of 24 individual experiments. *p < 0.05, **p < 0.01, ****p < 0.0001, and ns by Mann-Whitney *U* test.

(D) Representative histograms of control and CLL patient BM progenitors. The stained sample is colored red and the isotype is shown in blue (see also Figure S1). (E–H) Combined intranuclear flow cytometry data from control (n = 8) and CLL patient (n = 6) HSPCs was utilized in the cytofkit2 R package to generate UMAP plots. Each point in the UMAP represents a single cell.

(E) Contour plots of the UMAP architecture for all combined samples or separated into control or CLL patients.

Figure 1. *Continued*
(F) Colored overlay of control (teal) and CLL patient (red) HSPCs. The borders of five distinct regions are indicated and individually numbered. (G–H) Expression of PU.1, GATA-2, GATA-1, CD38, and CD45RA was superimposed on the cohort-specific architectures. Note that the data are normalized and expression values are relative to each individual factor.
See also Figures S1–S4.

CLL B cells (Manso et al., 2019; Sala et al., 1998; Tsopra et al., 2009). Thus, the mechanism(s) responsible for impaired BM hematopoiesis in CLL are likely multifactorial and, at present, largely unexplored.

CLL B cells constitutively produce multiple factors capable of modulating BM hematopoiesis, most prominently tumor necrosis factor alpha (TNFα) (Foa et al., 1990; Michalevicz et al., 1991). TNFα is elevated in patient plasma, and levels associate with disease progression (Bojarska-Junak et al., 2008). The role of TNFα in steady-state hematopoiesis is largely suppressive to maintain BM homeostasis and aberrant exposure can result in BM failure, cytopenias, and anemia, clinical complications often observed in late-stage CLL patients (Broxmeyer et al., 1986; Geissler et al., 1991; Means et al., 1990; Michalevicz et al., 1991; Skobin et al., 2000; Tian et al., 2014; Tsopra et al., 2009). Limited studies have shown that TNFα, in part, can alter TF expression levels in mouse and human hematopoietic progenitors to mediate these modulatory actions (Etzrodt et al., 2019; Grigorakaki et al., 2011). Our previous report was the first to assess this mechanism in the context of CLL where we showed that *in vitro* exposure of control human BM progenitors (aged-matched to CLL patients) to TNFα upregulated PU.1 and GATA-2 proteins, phenocopying *ex vivo* findings in CLL patient marrow (Manso et al., 2019). However, questions remain concerning *in vivo* sources of TNFα in CLL, developmental stage-specific HSPC subset sensitivity to direct CLL B cell exposure or their secreted factors, mechanisms of TNFα modulation of HSPC TF expression, and reversibility of TF alterations upon effective TNFα neutralization. This report details our new findings in relation to these questions at both a global and single-cell level as assayed in primary human BM hematopoietic progenitors from control subjects and CLL patients.

Results

Global and single-cell analysis of control and CLL patient bone marrow progenitors

GATA-2, PU.1, and GATA-1 are cell fate determinants directly modulated by TNFα in BM progenitors (Etzrodt et al., 2019; Grigorakaki et al., 2011). GATA-2 is critical for HSC maintenance and survival and has additional roles in determining erythroid, megakaryocyte, and granulocyte cell fates (Vicente et al., 2012). PU.1 and GATA-1 are master regulators of myeloid and erythroid cell fates, respectively (Burda et al., 2010). Importantly, these factors are cross-antagonistic and the relative abundance of each reinforces bifurcating lineage decisions (Walsh et al., 2002). Given the importance of these TFs in regulation of primitive hematopoiesis, and their modulation by TNFα(Etzrodt et al., 2019; Grigorakaki et al., 2011), we examined global expression levels of these TFs in developmental stage-specific hematopoietic stem and progenitor cell (HSPC) populations: HSC/multipotent (HSC/MPP, $Lin^{-}CD34^{hi}CD38^{-}CD45RA^{-}$), lymphoid-biased multipotential (LMPP, $Lin^{-}CD34^{hi}CD38^{-}CD45RA^{+}$), common myeloid/megakaryocyte-erythroid (CMP/MEP, $Lin^{-}CD34^{+}CD38^{+}CD45RA^{-}$), and granulocyte-monocyte (GMP, $Lin^{-}CD34^{+}CD38^{+}CD45RA^{+}$) progenitors (Figure S1).

Freshly isolated HSC/MPPs from CLL patient BM exhibited significantly increased protein levels of PU.1 and GATA-2 when evaluated by flow cytometry and compared with age-matched controls (Figures 1A and 1B), consistent with and extending our previous findings that were largely performed in cryopreserved patient samples among simplified progenitor cell fractions (Manso et al., 2019). Here, our refined analysis further revealed that CLL patient-derived LMPPs and CMP/MEPs exhibited significantly higher levels of PU.1 and GATA-2. GATA-2 was also elevated among CLL GMPs. In contrast, an increased frequency of $GATA\text{-}1^{+}$ cells was only observed in HSC/MPPs and CMP/MEPs (Figure S2), and those populations also display elevated levels of GATA-1 protein (among total $GATA\text{-}1^{+}$ cells, Figure 1C). Representative histograms of PU.1, GATA-2, and GATA-1 (shown in red) from control and CLL HSPCs compared with isotype controls (shown in blue) are displayed in Figure 1D.

TF expression levels exist along a dynamic spectrum at the single-cell level, and as a function of cellular differentiation, a feature global analysis of total cell fractions does not wholly represent. Therefore, we employed uniform manifold approximation and projection (UMAP) (Leland McInnes, 2018) dimensionality reduction across the totality of the four HSPC populations from controls and CLL patients to evaluate

alterations in TFs and/or phenotypic markers at the single-cell level. We reasoned that, because UMAP normalizes expression of clustering markers across the combination of each input sample, this analysis would allow for the relative relatedness of individual cells to be analyzed. This first-of-a-kind analysis of control and CLL HSPCs enabled us to define global architectures for each cohort and also capture TF alterations at the resolution of single cells (Figures 1E and S3A). As expected, control HSPCs displayed significant heterogeneity in their UMAP occupancy, reflecting a diversity of phenotypes. When overlaid, CLL HSPCs were found, differentially represented, within three distinct control phenotypes (Figure 1F, circled regions 1, 2 and 4), yet largely enrich into region 4. A subset of control HSPCs also uniquely occupied a third region (region 3), which CLL HSPCs were strikingly absent from. Interestingly, region 5 represents a unique population of HSPCs found in CLL BM only.

Using the UMAP architecture, we next visualized the relative expression of PU.1, GATA-2, and GATA-1 (normalized to each specific parameter) across control and CLL HSPCs (Figure 1G). Control HSPCs exhibited considerable PU.1 heterogeneity and moderately uniform, yet variable, GATA-2 and GATA-1 expression. CLL HSPCs exhibited increased expression heterogeneity across all three TFs. When individual regions were evaluated, region 1 displayed variable PU.1 expression and high levels of GATA-2 and GATA-1. CLL HSPCs in region 1 were found to exhibit similar PU.1 and GATA-2 expression patterns as control HSPCs but have a distinct increase in GATA-1 positivity (Figures 1G and S4). Control HSPCs in region 2, a smaller region also occupied by CLL HSPCs, was characterized by low levels of PU.1, intermediate levels of GATA-2, and low levels of GATA-1. CLL HSPCs in region 2 show comparable PU.1 and GATA-2 expression patterns compared with controls, yet there is a small population of PU.1^{hi} cells. CLL HSPCs in this region also display increased GATA-1 expression. The unique control HSPC region 3 is composed of GATA-2^{hi} cells that also express the highest control HSPC levels of PU.1 and GATA-1. Region 4, a CLL-enriched group sharing marginal overlap with controls, displayed variable expression of GATA-2 and low levels of PU.1 and GATA-1 in control HSPCs. In contrast, CLL HSPCs in region 4 exhibit increased yet bimodal expression of PU.1 and GATA-2 and very low levels of GATA-1. Finally, the CLL-enriched region 5 is comprised of cells with low levels of all three TFs.

The cell surface markers CD38 and CD45RA are utilized to distinguish human HSPC subsets (Figures 1H and S4). When assessed by UMAP analysis, significant heterogeneity of CD38 and CD45RA expression was observed in control and CLL HSPCs. Regions 1 and 2 are enriched for cells with higher expression of CD38 and low/intermediate CD45RA. Control HSPCs in region 3 are characterized by intermediate levels of CD38 and increased, although variable, CD45RA expression. Both control and CLL HSPCs exhibit variable CD38 expression in the CLL-enriched region 4. Interestingly, control HSPCs in region 4 show bimodal CD45RA expression, whereas CLL HSPCs are largely CD45RA^{low}. In contrast, the CLL-specific region 5 displays a unique signature of CD38^{low} levels and uniformly high expression of CD45RA. Together, these data demonstrate that CLL BM HSPCs are distinct from controls and express fundamentally altered TF and cell surface marker profiles when assessed globally and at the single cell level.

CLL cells modulate TF protein levels in specific BM HSPC subsets

CLL B cells constitutively produce soluble and membrane-bound factors that may impact normal hematopoiesis (Burger et al., 2009; Foa et al., 1990; Janel et al., 2014; Kay et al., 2002; Lahat et al., 1991; Lotz et al., 1994; Saulep-Easton et al., 2016; van Attekum et al., 2017). Therefore, we sought to test if CLL cells modulate PU.1, GATA-2, and GATA-1 expression levels in HSPC subsets via cell contact and/or secreted/soluble factors by comparing direct and Transwell co-cultures consisting of primary CLL cells and age-matched control Lin$^-$CD34$^+$ HSPCs. To establish an experimental ratio of CLL B cells:control HSPCs, we assessed the cellular ratio of CD19$^+$CD5$^-$ and CD19$^+$CD5$^+$ B cells to Lin$^-$CD34$^+$ HSPCs in control and CLL BM (Figure S5). As expected, the ratio was orders of magnitude higher in CLL patients compared with controls. A 10:1 (CLL cells:HSPCs) ratio was used in all *in vitro* experiments for two reasons. First, it is reasonably greater than control CD19$^+$CD5$^+$ B cell to HSPC ratios. Second, it allows for evaluation of CLL B-cell-induced alterations in an environment mimicking lower thresholds of leukemic marrow infiltration as would be predicted in early stage disease.

Following 24 h of short-term co-culture allowing direct contact between control HSPCs and primary CLL B cells, the HSC/MPP, LMPP, CMP/MEP, and GMP populations were evaluated for levels of PU.1, GATA-2, and GATA-1 by flow cytometry. We note that the co-culture is serum free, eliminating any contribution of serum-derived factors in TF modulation. Short-term direct exposure to CLL cells significantly increased

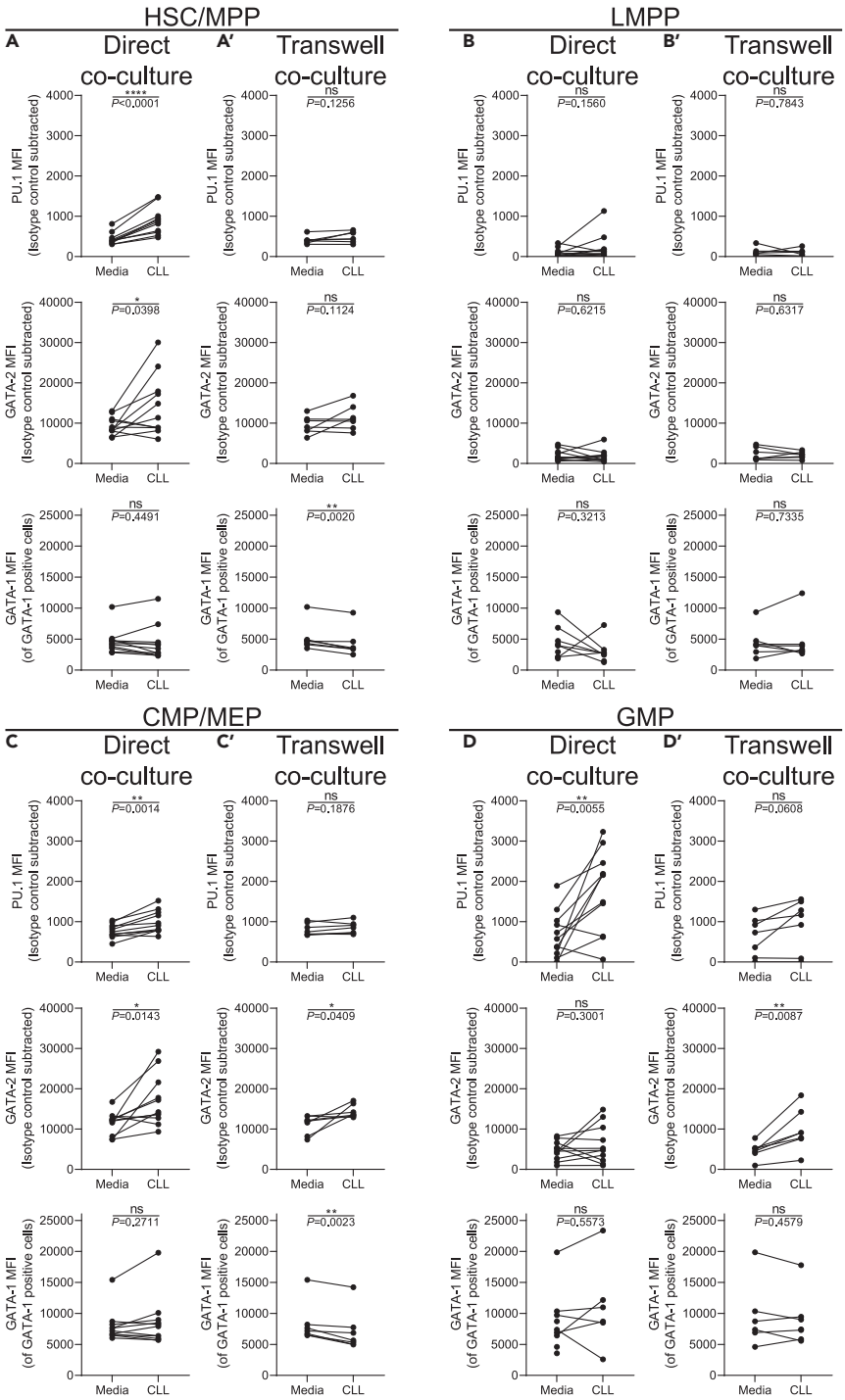

E

	HSC/MPP		LMPP		CMP/MEP		GMP	
	Cell-cell Direct co-culture	Soluble TransWell co-culture	Cell-cell Direct co-culture	Soluble TransWell co-culture	Cell-cell Direct co-culture	Soluble TransWell co-culture	Cell-cell Direct co-culture	Soluble TransWell co-culture
PU.1 MFI	↑	---	---	---	↑	---	↑	---
GATA-2 MFI	↑, Variable	---	---	---	↑, Variable	↑	---	↑
GATA-1 MFI	---	↓	---	---	---	↓	---	---

Figure 2. Expression of PU.1, GATA-2, and GATA-1 are modulated *in vitro* by direct co-culture with CLL B cells

(A–D′) Freshly isolated control BM $CD34^+$ cells were cultured in media alone, (A–D) directly with peripheral blood CLL cells, or (A′–D′) indirectly by use of a 1.0 μm Transwell insert at a ratio of 10:1 (CLL cells:HSPCs) for 24 h. Flow cytometry was performed to determine the MFI (indicative of relative protein levels) of PU.1, GATA-2, and GATA-1 among (A and A′) $Lin^-CD34^{hi}CD38^-CD45RA^-$ HSC/MPPs, (B and B′) $Lin^-CD34^{hi}CD38^-CD45RA^+$ LMPPs, (C and C′) $Lin^-CD34^+CD38^+CD45RA^-$ CMP/MEPs, and (D and D′) $Lin^-CD34^+CD38^+CD45RA^+$ GMPs. Each point represents a unique pairing of a control HSPC donor and CLL patient, with lines connecting the pairs (n = 11 for direct co-culture and n = 7 for Transwell co-cultures, 11 individual experiments). *p < 0.05, **p < 0.01, ****p < 0.0001, and ns by paired t test. (E) Summary table of the *in vitro* co-culture results. Changes to expression of each TF is indicated by ↑ = increased, ↓ = decreased, and — = no change.

See also Figures S5 and S8.

PU.1 and GATA-2 in HSC/MPPs without affecting levels of GATA-1 compared with HSC/MPPs cultured in media alone (Figure 2A). Similarly, PU.1 was upregulated in the CMP/MEP and GMP (Figures 2C and 2D), but not LMPP, subsets (Figure 2B). In addition to HSC/MPPs, GATA-2 was also increased among CMP/MEPs. Interestingly, GATA-2 displayed a variable response, with some control HSC/MPPs and CMP/MEPs not affected by the co-culture (Figures 2A and 2C). GATA-1 remained unchanged in all populations. These new findings indicate that direct short-term co-culture of CLL B cells with control HSPCs differentially alters TF expression levels across multiple transitional stages of hematopoietic differentiation.

Next, we asked whether the TF alterations required direct contact between control HSPCs and CLL B cells or if modulation could be mediated by soluble factors provided by the CLL cells. To test this possibility, we physically separated the CLL B cells from control HSPCs by using Transwell inserts during the short-term co-culture. In contrast to the results obtained in the direct co-cultures, HSPCs separated from CLL cells showed no significant change in PU.1 in any population examined (Figures 2A′–2D′). GATA-2 remained unchanged in HSC/MPPs and LMPPs but significantly increased in CMP/MEPs and GMPs, indicating differential TF sensitivity of individual progenitor stages to CLL-derived soluble factors (Figures 2C′–2D′). HSC/MPPs and CMP/MEPs, but not LMPPs or GMPs, exhibited a decline in GATA-1 levels. Together, these findings suggest differential requirements for direct CLL:HSPC cell contact versus CLL-derived soluble factors in modulation of PU.1, GATA-2, and GATA-1 within developmental stage-specific HSPC subsets (summarized in Figure 2E).

CLL-derived TNFα directly modulates PU.1 and GATA-2 expression

In our previous study we reported that exogenous TNFα rapidly increased expression of PU.1 and GATA-2 in control HSPCs (Manso et al., 2019). We have extended these findings and determined that TNFα exposure reduces levels of GATA-1, consistent with previously published data (Buck et al., 2009; Grigorakaki et al., 2011) (Figure S6A). Further, NF-κB p65 (RelA), a TF at the nexus of inflammatory and TNFα signaling cascades (Liu et al., 2017; Nakagawa et al., 2018), is overexpressed in CLL-derived HSC/MPPs, unchanged in LMPPs and CMP/MEPs, and reduced in GMPs (Figure S7). We also note that the effects of TNFα on human HSPCs may be long-lasting or irreversible (Dybedal et al., 2001). TNFα is constitutively produced by CLL B cells in both membrane-bound and soluble forms (Foa et al., 1990; Michalevicz et al., 1991). Furthermore, TNFRI and TNFRII are expressed on primitive human HSPCs (Wang et al., 2017). To determine if TNFα derived from CLL B cells contributes to the alterations in PU.1, GATA-2, and GATA-1 in control HSPCs, a specific neutralizing antibody against TNFα (anti-TNFα) (Kim et al., 2018; Rothhammer et al., 2018) was added to the short-term direct and Transwell CLL:control HSPC co-cultures. Addition of anti-TNFα to the direct co-cultures significantly reduced levels of PU.1 in HSC/MPP, CMP/MEP, and GMP populations (Figures 3A, 3B, and 3D). GATA-2 was reduced in HSC/MPPs and CMP/MEPs but not GMPs. As PU.1 and GATA-2 were not modulated in LMPPs in the direct co-culture (Figure 2B), they remained unchanged when TNFα was neutralized (Figure 3B). Interestingly, GATA-1 protein levels were increased in HSC/MPPs and LMPPs upon neutralization of TNFα.

In contrast to the direct co-culture results, anti-TNFα did not significantly alter PU.1 levels in HSC/MPPs, LMPPs, or CMP/MEPs in Transwell cultures (Figure 3A′–C′), which was expected, as CLL-derived soluble factors alone did not alter PU.1 expression. However, a reduction in PU.1 was observed in GMPs (Figure 3D′). GATA-2 expression was reduced in HSC/MPPs and CMP/MEPs in Transwell cultures supplemented with anti-TNFα (Figure 3A′ and 3C′). Neutralizing TNFα did not alter GATA-2 levels in LMPPs or GMPs (Figure 3B′ and 3D′). This was expected of LMPPs, as they were refractory to CLL-derived soluble factors in the Transwell culture. The unchanging levels of GATA-2 in GMPs suggest a TNFα-independent

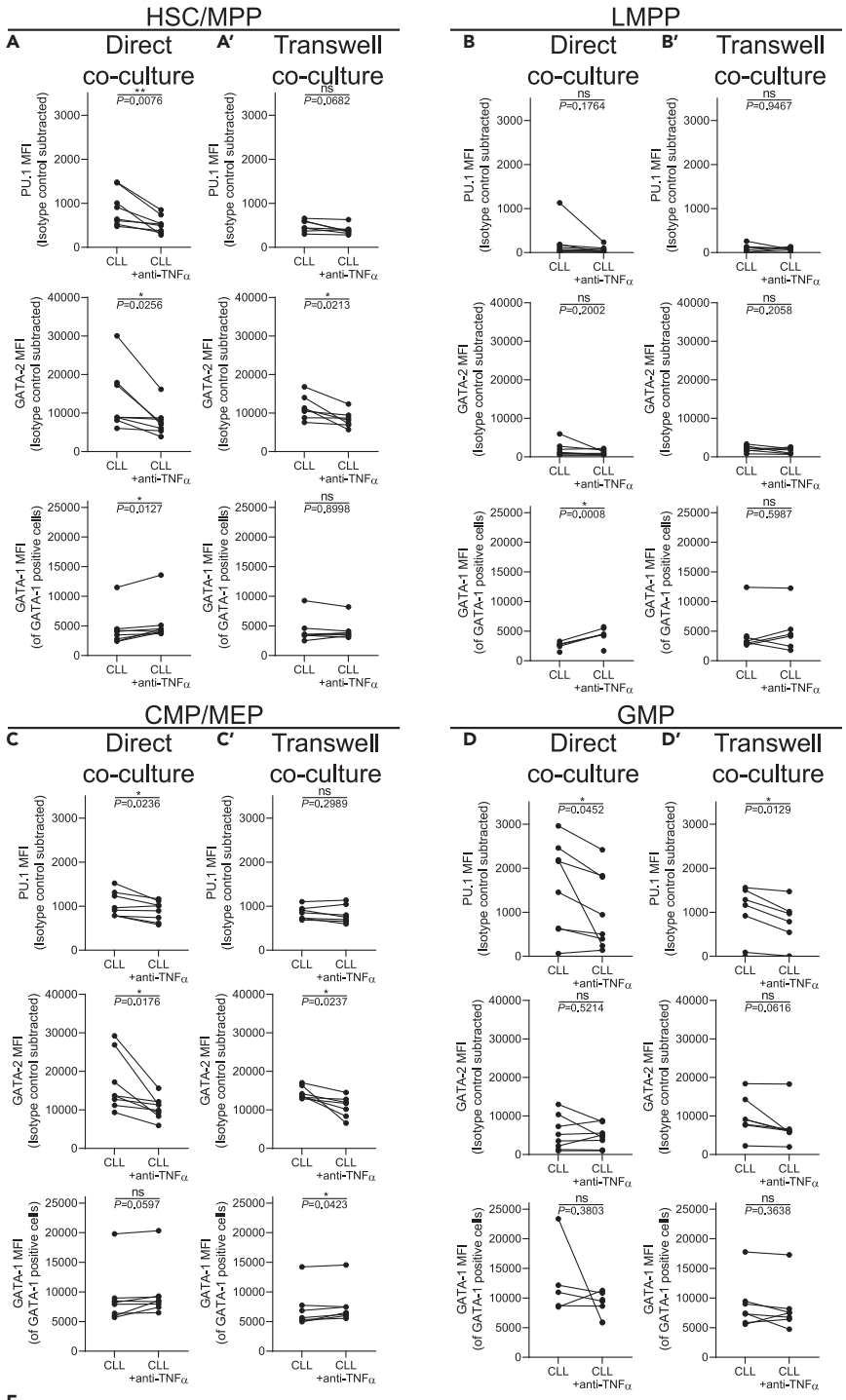

E

	HSC/MPP		LMPP		CMP/MEP		GMP	
	Cell-cell Direct co-culture	Soluble TransWell co-culture	Cell-cell Direct co-culture	Soluble TransWell co-culture	Cell-cell Direct co-culture	Soluble TransWell co-culture	Cell-cell Direct co-culture	Soluble TransWell co-culture
PU.1 MFI	↓	---	---	---	↓	---	↓	↓
GATA-2 MFI	↓, Variable	↓	---	---	↓, Variable	↓, Variable	---	---
GATA-1 MFI	↑	---	↑	---	---	↑	---	---

Figure 3. CLL B-cell-derived TNFα modulates transcription factor expression levels *in vitro*

(A–D′) Freshly isolated control BM $CD34^+$ cells were cultured in the presence or absence of a neutralizing antibody against TNFα (anti-TNFα) either (A–D) directly with peripheral blood CLL cells or (A′–D′) indirectly cultured by use of a 1.0 μm Transwell insert at a ratio of 10:1 (CLL cells:HSPCs) for 24 h. Flow cytometry was performed to determine the MFI (indicative of relative protein levels) of PU.1, GATA-2, and GATA-1 among (A, A′) $Lin^-CD34^{hi}CD38^-CD45RA^-$ HSC/MPPs, (B and B′) $Lin^-CD34^{hi}CD38^-CD45RA^+$ LMPPs, (C and C′) $Lin^-CD34^+CD38^+CD45RA^-$ CMP/MEPs, and (D and D′) $Lin^-CD34^+CD38^+CD45RA^+$ GMPs. Each point represents a unique pairing of a control HSPC donor and CLL patient, with lines connecting the pairs (n = 8 for direct co-culture and n = 7 for Transwell co-cultures, 8 individual experiments). *$p < 0.05$, **$p < 0.01$, and ns by paired t test.

(E) Summary table of the *in vitro* co-culture results. Changes to expression of each TF is indicated by ↑ = increased, ↓ = decreased, and — = no change.

See also Figures S5, S6, and S8.

effect for GATA-2 modulation in this population. GATA-1 protein remained unchanged upon neutralization of TNFα in all subsets except CMP/MEPs, where it was elevated (Figure 3C′). The effects of anti-TNFα *in vitro* are summarized in Figure 3E. Importantly, complete normalization of PU.1, GATA-2, and GATA-1 was observed when anti-TNFα was added to recombinant TNFα-exposed control progenitors, confirming effective TNFα neutralization in the co-culture model (Figure S6B).

We next compared media controls with direct CLL B cell:HSPC co-cultures that were subjected to TNFα neutralization to further investigate TNFα-specific modulation (Figure S8A). Compared with media controls, neutralization of TNFα normalized PU.1 in all populations except CMP/MEPs, where PU.1 remained slightly elevated. Anti-TNFα completely restored GATA-2 to control levels in all progenitor subsets except LMPPs, where it was slightly decreased. Notably, although direct co-culture did not change GATA-1 levels, neutralization of TNFα slightly elevated GATA-1 in CMP/MEPs.

When the same comparisons were made in Transwell co-cultures (Figure S8B), no changes were observed in PU.1. However, GATA-2 was slightly decreased in HSC/MPPs and restored in LMPPs, CMP/MEPs, and GMPs. GATA-1 also demonstrated differential responses. GATA-1 was reduced among HSC/MPP and CMP/MEP, but not LMPP and GMP, progenitors. Together, these data demonstrate that CLL B-cell-derived TNFα directly modulates aberrant expression of PU.1 and GATA-2 (and to a lesser extent GATA-1) in BM HSPCs. Further, given that complete TNFα neutralization does not restore every population to media control levels, other CLL-derived factors are likely contributing to TF modulation in BM progenitor cells.

Single-cell analysis of CLL:HSPC co-cultures reveal distinct mechanisms of TF modulation in HSPCs by CLL B cells

To investigate HSPC population changes in our co-culture model at the single-cell level, we performed UMAP analysis collectively of all *in vitro* experiments (Figures 4 and S3B). The general single-cell distribution of the media controls revealed segregation into three distinct regions that were largely maintained across all experimental conditions. However, unique variations to the overall UMAP architecture were induced by individual experimental manipulations. Next, we assessed the relative expression profiles of PU.1, GATA-2, and GATA-1 across the *in vitro* UMAP architecture for each experimental condition. Overall, the media controls exhibited high heterogeneity. The *in vitro* UMAP region 1 exhibited low levels of PU.1 and GATA-1 with intermediate levels of GATA-2. The second region displayed high levels of PU.1 and GATA-2, with lower, yet varying, levels of GATA-1. The third region was comprised of high levels of GATA-2 and GATA-1 with lower levels of PU.1. Addition of recombinant TNFα shifted control progenitors into regions with high levels of PU.1 and GATA-2 with variable, yet declining, GATA-1 expression. When the recombinant TNFα was neutralized, virtually identical UMAP architecture and TF patterning was observed when compared with the media controls.

Direct co-culture with CLL cells shifted control HSPCs to a unique signature of highly variable TF expression (Figure 4). Of note, the majority of cells in this culture condition expressed high levels of PU.1 and GATA-2 while maintaining a similar GATA-1 signature compared with media controls. Interestingly, the signature adopted when TNFα was neutralized in the CLL direct co-culture maintained regions of high PU.1 and GATA-2 expression, yet with a different cellular distribution among the UMAP architecture. The bimodal expression of GATA-1 was maintained. When CLL-derived soluble factors were evaluated in Transwell co-cultures, another unique signature was observed. Compared with media controls, relative levels of PU.1 were increased while GATA-2 and GATA-1 were maintained. Neutralization of TNFα in the Transwell

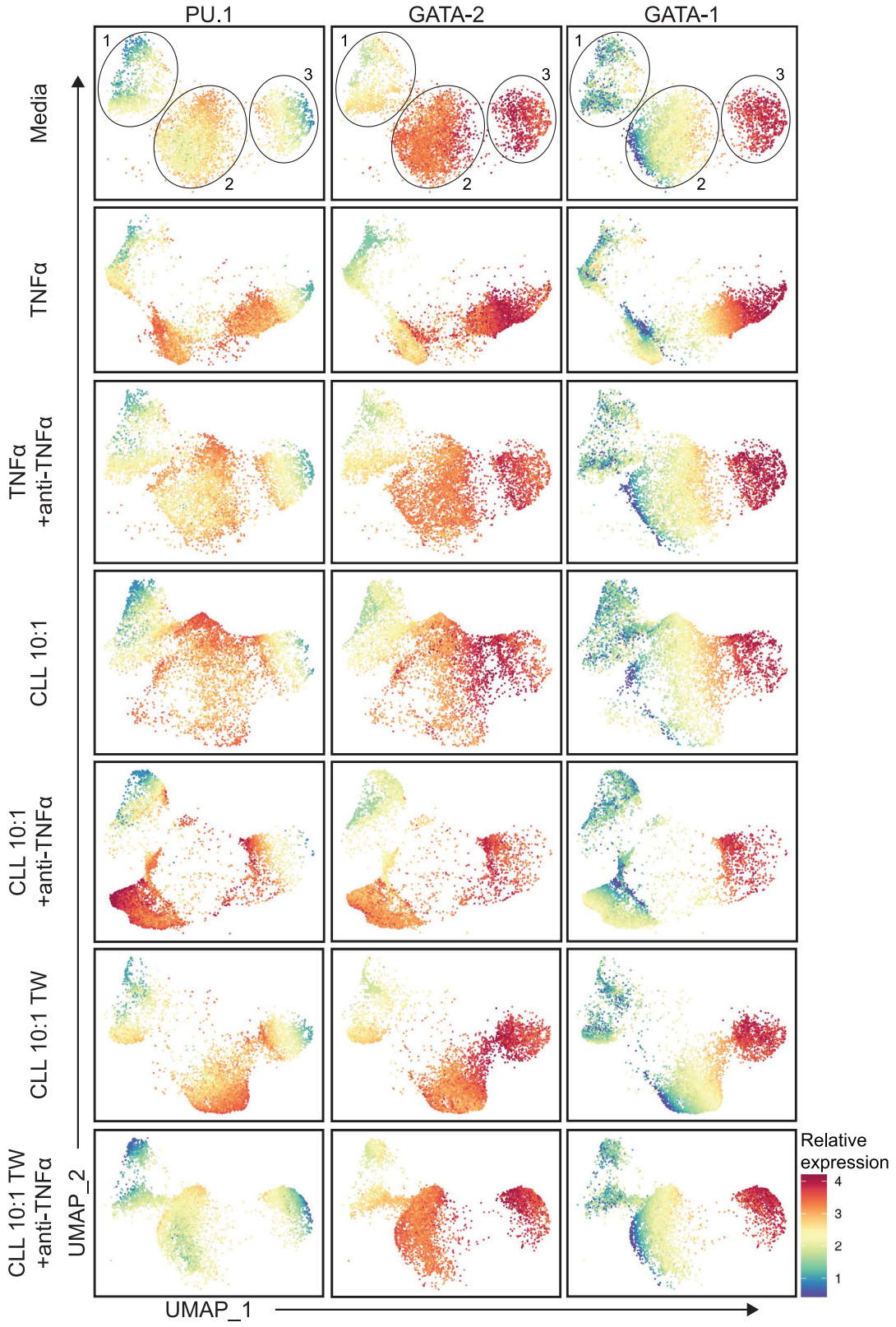
PU.1
GATA-2
GATA-1
Media
TNFα
TNFα +anti-TNFα
CLL 10:1
CLL 10:1 +anti-TNFα
CLL 10:1 TW
CLL 10:1 TW +anti-TNFα
1
2
3
UMAP_2
UMAP_1
Relative expression
4
3
2
1

Figure 4. Single-cell UMAP analysis of HSPC expression of PU.1, GATA-2, and GATA-1 induced by CLL B cell direct or Transwell co-culture

The relative expression of PU.1, GATA-2, and GATA-1 was overlaid on each individual media (n = 20), TNFα (n = 10), TNFα+anti-TNFα (n = 6), CLL direct co-culture (n = 12), CLL + anti-TNFα direct co-culture (n = 9), CLL Transwell (TW) co-culture (n = 7), and CLL + anti-TNFα TW co-culture (n = 7) *in vitro* condition UMAP. The expression values and colors of each factor are normalized and relative to themselves. Each point in the UMAP represents a single cell and the total data are comprised of 20 individual experiments.

co-cultures largely restored control HSPC TF expression to that of the media control signature, although slight differences were observed, such as an overall reduction in PU.1 levels. Collectively, the UMAP analysis of the *in vitro* co-culture conditions revealed distinct alterations in the expression of PU.1, GATA-2, and GATA-1 at the single-cell level. Furthermore, direct CLL B cell:HSPC contact versus exposure to CLL soluble factors induced distinct TF signatures within specific HSPC populations and at the single-cell level.

Partial restoration of myelopoiesis upon removal of HSCs from the leukemic bone marrow microenvironment

We previously reported reduced frequencies and functional impairment of BM HPSCs analyzed immediately *ex vivo* from untreated CLL patients (Manso et al., 2019). We next sought to determine if the cell-intrinsic functional defect documented in the CLL HSPCs analyzed *ex vivo* was reversible with prolonged removal from the leukemic microenvironment. To make this determination, we utilized the long-term culture initiating cell (LTC-IC) assay (Liu et al., 2013) to test the ability of control and CLL-derived HSCs to initiate and sustain myelopoiesis for 5 weeks across serial input cell concentrations (Figure 5A). As determined by frequencies of wells containing clonal progeny, we observed that CLL myeloid-biased HSCs generated significantly fewer clonal progeny, particularly early in the culture period. This finding is likely a result of maintaining biologic alterations incurred from their *in vivo* exposure to CLL B cell contact, secreted factors, or other features of a CLL-modified microenvironment. Interestingly, some individual CLL donor HSCs recovered functional capacity and were indistinguishable from controls by weeks 4–5 of culture, although the overall response remained diminished. Notably, this effect was not a function of altered $CD34^+$ isolation purity between controls and CLL patients (Figure 5B). Importantly, when limiting dilution analysis (LDA) was performed (Hu and Smyth, 2009), a near 2-fold decrease in myelopoiesis-potentiating HSC precursor frequency was observed among CLL patients (Figures 5C and 5D).

Chronic exposure to TNFα reduces myeloid-biased HSC clonality

Given the impact of TNFα on progenitor TF profiles that regulate myelopoiesis, we next determined the contribution of TNFα to myeloid dysfunction. Confirming previous reports (Broxmeyer et al., 1986; Geissler et al., 1991; Skobin et al., 2000), addition of TNFα to CFU assays significantly reduced colony formation, which was restored when TNFα was neutralized (data not shown). Given these findings, we wished to determine if chronic exposure to TNFα would recapitulate the functional decrease of CLL-derived myeloid HSCs. As it is difficult to experimentally mimic the exact local *in vivo* TNFα concentrations in CLL patient BM HSPC niches, we performed a dilution series of TNFα in the LTC-IC assay with control BM HSPCs. As previously reported for $CD34^+CD38^-$ hematopoietic progenitors (Dybedal et al., 2001; Maguer-Satta et al., 2000; Petzer et al., 1996), chronic TNFα exposure of control HSPCs resulted in a dose-dependent inhibition of myelopoiesis (Figure 5E). Interestingly, chronic low-dose exposure effects were more prominent at early culture time points and resolved over time. Importantly, the TNFα-induced reduction in clonal progeny recapitulated the diminished *ex vivo* CLL functional responses shown in Figure 5A. These data further reinforce a role for TNFα in diminishing myelopoiesis in CLL patient BM.

Discussion

Here, we report a mechanism for diminished BM myelopoiesis in CLL patients driven by leukemic B-cell-derived TNFα. Combining *ex vivo* and *in vitro* experimental findings, we show that CLL B cells directly modulate PU.1 and GATA-2 expression in BM HSCs and myelo-erythroid progenitor subsets at the single-cell level. We pursued mechanisms of TF modulation and found that TNFα, produced by the CLL clone, plays an integral role. Importantly, short-term TNFα modulation of PU.1 and GATA-2 is reversible as neutralization of TNFα normalized changes in expression of PU.1 and GATA-2 induced by CLL cells. CLL is a chronic disease and BM infiltration is found even in early stage patients. We determined that removal of HSCs from the leukemic BM microenvironment restored myelopoietic function, although numbers of myeloid-biased HSCs were significantly reduced. Building on this observation, we show that chronic *in vitro* exposure of control age-matched HSPCs to a range of TNFα concentrations, including low dose and approximating levels reported to be produced by CLL B cells *in vitro*(Rosati et al., 2005), reduced

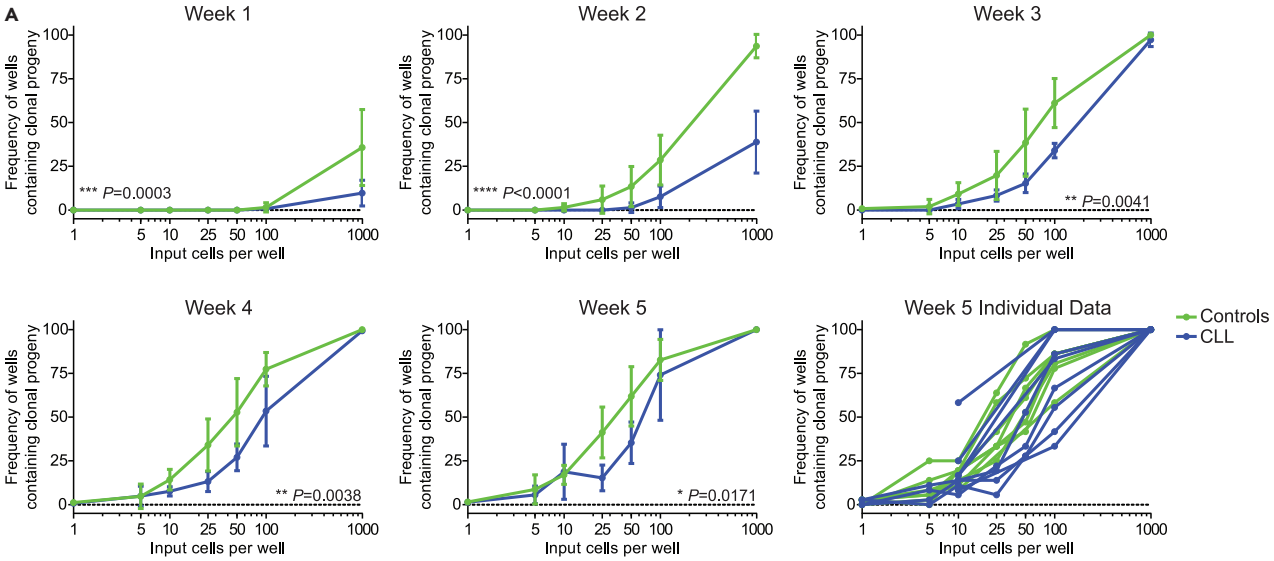

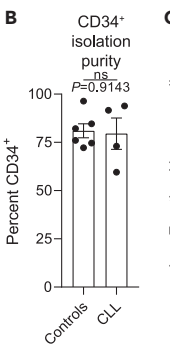

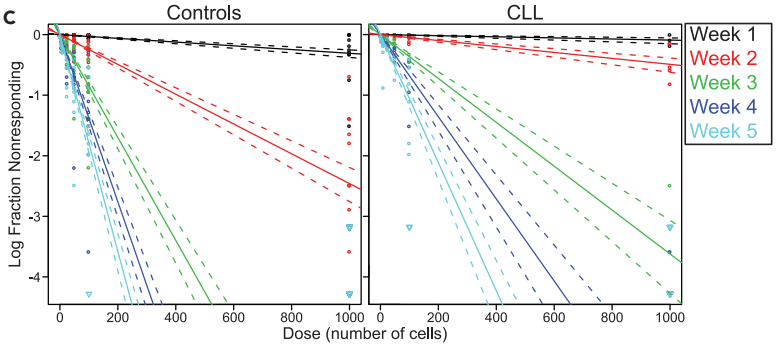

D

	Limiting Dilution Analysis 1/(stem cell frequency) Estimates	
	Controls	CLL
Week 1	3239.7	10957
Week 2	406.6	2038
Week 3	117.7	276.2
Week 4	72.5	147.5
Week 5	55.9	94.6

	Estimate value fold difference (CLL/Controls)
Week 1	3.4
Week 2	5.0
Week 3	2.3
Week 4	2.0
Week 5	1.7

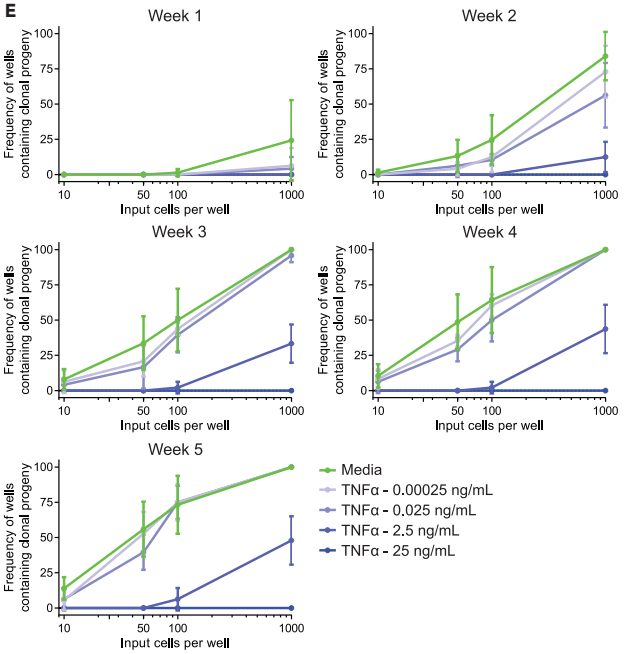

Week 1

TNFα (ng/mL)	Media	P value summary (adjusted P value)			
0.00025	ns (0.4256)				
0.025	ns (0.3216)	ns (0.9998)			
2.5	ns (0.1633)	ns (0.9890)	ns (0.9977)		
25	ns (0.1633)	ns (0.9890)	ns (0.9977)	ns (>0.9999)	
	Media	0.00025	0.025	2.5	25
		TNFα (ng/mL)			

Week 2

TNFα (ng/mL)	Media	P value summary (adjusted P value)			
0.00025	ns (0.0882)				
0.025	** (0.0024)	ns (0.8073)			
2.5	**** (<0.0001)	**** (<0.0001)	** (0.0014)		
25	**** (<0.0001)	**** (<0.0001)	**** (<0.0001)	ns (0.9227)	
	Media	0.00025	0.025	2.5	25
		TNFα (ng/mL)			

Week 3

TNFα (ng/mL)	Media	P value summary (adjusted P value)			
0.00025	ns (0.5191)				
0.025	ns (0.0673)	ns (0.8746)			
2.5	**** (<0.0001)	**** (<0.0001)	**** (<0.0001)		
25	**** (<0.0001)	**** (<0.0001)	**** (<0.0001)	ns (0.1511)	
	Media	0.00025	0.025	2.5	25
		TNFα (ng/mL)			

Week 4

TNFα (ng/mL)	Media	P value summary (adjusted P value)			
0.00025	ns (0.6293)				
0.025	ns (0.0525)	ns (0.7567)			
2.5	**** (<0.0001)	**** (<0.0001)	**** (<0.0001)		
25	**** (<0.0001)	**** (<0.0001)	**** (<0.0001)	* (0.0370)	
	Media	0.00025	0.025	2.5	25
		TNFα (ng/mL)			

Week 5

TNFα (ng/mL)	Media	P value summary (adjusted P value)			
0.00025	ns (0.9283)				
0.025	ns (0.4870)	ns (0.9084)			
2.5	**** (<0.0001)	**** (<0.0001)	**** (<0.0001)		
25	**** (<0.0001)	**** (<0.0001)	**** (<0.0001)	** (0.0082)	
	Media	0.00025	0.025	2.5	25
		TNFα (ng/mL)			

Figure 5. CLL HSPCs are functionally compromised, and the dysfunction is recapitulated by exposure to TNFα

(A) $CD34^+$ HSPCs were isolated from control (green) and CLL (blue) BM and plated in the long-term culture initiating cell (LTC-IC) assay under limiting dilution conditions (12 or 36 replicates per dilution). Cultures were evaluated weekly for presence of clonal progeny (as evidenced by the occurrence of at least one colony). Data are presented as the mean ± SD frequency of wells containing clonal progeny. Weeks 1–4 represent n = 4 for both controls and CLL, with week 5 data containing n = 8 controls and n = 9 CLL donors across 18 individual experiments. *p < 0.05, **p < 0.01, ***, p < 0.001, and ****p < 0.0001 by two-way ANOVA.

(B) When available, surplus isolated $CD34^+$ cells (see Transparent methods) were tested by flow cytometry for purity (Control n = 6, CLL n = 4). ns by Mann-Whitney *U* test. Due to the reduced frequency of $CD34^+$ cells in CLL BM (Manso et al., 2019) and limiting volumes of fresh BM, not every donor was able to be evaluated.

(C) Limiting dilution analysis (LDA) was performed at each time point for control and CLL LTC-IC assays to estimate numbers of responding HSCs among the input $CD34^+$ cells. Circles indicate individual data points, with downward-facing triangles representing a negative (zero) response. Solid lines are the dilution model's fit, with dashed lines indicating the 95% confidence interval. Each time point is represented by a unique color as indicated.

(D) LDA estimates of 1/(stem cell frequency) for control and CLL HSPCs at each time point and fold difference in estimated precursor cell frequency.

(E) LTC-IC assays were performed at limited cell dilutions (12 replicates each) of control BM HSPCs with media alone or supplemented with the indicated concentrations of TNFα. Cells were scored weekly as in (A). Data are presented as the mean ± SD frequency of wells containing clonal progeny at each time point and dilution. n = 4 and is representative of three individual experiments. Statistical comparisons between each dilution at each time point are indicated in the accompanying data tables. *p < 0.05, **p < 0.01, ****p < 0.0001, and ns by two-way ANOVA adjusted for multiple comparisons (Tukey).

the numbers and function of myeloid-biased HSCs, largely mimicking CLL patient clinical data. The experimental findings detailed herein provide new insight into the basis of BM hematopoietic dysfunction in CLL patients that likely contribute to impaired immune status.

Our study highlights CLL B-cell-derived TNFα as a major driver of impaired BM myelopoiesis in CLL patients. We focused on TNFα, as it is constitutively produced by CLL B cells (Foa et al., 1990; Michalevicz et al., 1991), has a well-described role in modulating myelopoiesis (Buck et al., 2009; Dybedal et al., 2001; Grigorakaki et al., 2011; Tian et al., 2014), and is implicated in CLL disease progression (Bojarska-Junak et al., 2008). TNFα is produced in two trimeric forms, soluble and membrane-bound, each of which preferentially binds to either TNF receptor 1 or TNF receptor 2 (TNFRI and TNFRII), respectively (Grell et al., 1995). Signaling through both TNF receptors is required for HSC regulation (Grell et al., 1995; Pronk et al., 2011), a critical consideration in Transwell cultures, where membrane-bound TNFα-TNFRII interaction is inhibited, resulting in differential responses compared with direct co-culture. Although we cannot discount the complex combinatorial effects that multiple cell-cell contacts and/or soluble mediators between CLL B cells and HSPCs may have, the reversal of PU.1 and GATA-2 protein elevation by anti-TNFα strongly implicate TNFα in mediating, at least in part, CLL-induced impaired myelopoiesis. Further, when the *in vitro* cultures and CFU assays were performed with interleukin-10 (IL-10), another cytokine constitutively produced by CLL B cells that is elevated in patient serum (DiLillo et al., 2013; Fayad et al., 2001) and has HSC modulating activity (Kang et al., 2007), no alterations were observed, further demonstrating the specific activity of CLL-derived TNFα (Figure S9). Lastly, the alterations in myelopoiesis we document do not require remodeling of the BM microenvironment, as the changes in expression levels of PU.1 and GATA-2 could be reproduced in short-term *in vitro* co-cultures comprised of CLL B cells and normal HSPCs that were devoid of stromal and other niche supportive cells.

In CLL patient BM, the hematopoietic dysfunction we show is associated with elevated levels of PU.1, GATA-2, and GATA-1 simultaneously in specific HSPC subsets at the single-cell level. Signaling pathways activated by cytokines influence cell fate trajectories by modulating the activity and/or expression levels of lineage-determining TFs. Here, we focused on TNFα, as levels of this cytokine are elevated in CLL BM (Bojarska-Junak et al., 2008) and CLL-related anemia has been shown to be strongly linked to TNFα(Tsopra et al., 2009). Our *in vitro* direct CLL B cell:control HSPC co-culture model showed increased PU.1 expression in primitive HSC/MPPs via CLL-derived TNFα. GATA-2 represses the GATA-2/GATA-1 switch critical for erythroid commitment (Bresnick et al., 2012; Moriguchi and Yamamoto, 2014) and was also elevated in progenitors exposed to CLL-derived TNFα. It is well established that overexpression of PU.1 or GATA-2 is disruptive for proper erythroid lineage commitment (Grigorakaki et al., 2011). GATA-2 can also directly antagonize PU.1 (Walsh et al., 2002; Zhang et al., 2000), suppressing myelopoiesis. We show, for the first time, that direct contact between CLL cells and HSPCs is likely required *in vivo* to increase HSPC expression levels of PU.1 via TNFα, as the PU.1 levels were normalized upon TNFα neutralization. Similarly, we found that CLL B cell direct contact and, to a certain extent, CLL B cell soluble factors (including TNFα), can upregulate GATA-2. Collectively, simultaneously increased levels of PU.1, GATA-2, and GATA-1 may antagonize erythroid and myeloid cell fate programs (Arinobu et al., 2007; Bresnick et al., 2012; Burda et al., 2010; Moriguchi and Yamamoto, 2014; Walsh et al., 2002; Wolff and Humeniuk, 2013), subverting lineage

commitment and differentiation, resulting in diminished mature blood cell output from the BM resulting in cytopenias and diminished immune competence.

To further understand the biology of BM hematopoiesis in CLL we also examined *ex vivo* phenotypic changes among control and CLL HSPCs at the single-cell level using UMAP dimensionality reduction. Distinct global architectures were observed that demonstrated that CLL-derived BM HSPCs are distinct from healthy controls and express fundamentally altered TF and cell surface marker profiles. Intriguingly, the CLL-enriched UMAP region 4 displayed high levels of CD38 with intermediate and variable CD45RA expression, phenotypically overlapping with CMP/MEPs. CLL HSPCs in region 4 also express higher levels of PU.1 and GATA-2 globally and at the single-cell level. We hypothesize that the phenotypic CMP/MEPs may be unable to resolve developmental transitions due to cross-antagonism between TFs. Conversely, the CLL-specific UMAP region 5 displayed a unique expression pattern of low CD38 and high CD45RA, phenotypically representative of LMPPs. Interestingly, this population displays low levels of PU.1, GATA-2, and GATA-1. Given that region 5 is notably enriched in our untreated CLL cohort, and does not express TFs indicative of myeloid or erythroid fates, it is tempting to speculate that this region is enriched for cells that are a CLL stem cell, a CLL-modified LMPP population, and/or a population protected from CLL-induced cellular reductions and is therefore overrepresented.

This study provides, for the first time, a unique and targetable mechanism by which CLL cells negatively regulate BM myelopoiesis. Investigation of mechanisms set a framework for designing interventions that could ameliorate clinically important cytopenias that strongly impact immune competency and clinical outcomes. Importantly, our study challenges the existing paradigm of peripheral immunosuppression as the only mechanism inducing immune cell dysfunction in CLL patients. Together, these new findings explain, in part, the etiology of cytopenias in CLL, particularly of the myelo-erythroid lineage (Manso et al., 2019; Zent et al., 2008). Advances in understanding BM hematopoietic dysfunction in CLL patients offers targetable mechanism(s) for the treatment and reversal of CLL-induced cytopenia and accompanying immunosuppression.

Limitations of the study

A caveat of this study is that it relied on the utilization of freshly prepared, untreated CLL samples and each individual CLL patient sample to be co-cultured with unique control donor HSPCs collected on the same day. This unavoidable constraint imposed by the availability of human experimental research material impaired our ability to further stratify results by clinically relevant CLL patient features (Table S1). We did not measure soluble TNFα levels in the co-cultures. TNFα levels in BM plasma are significantly higher than blood plasma and correlate with disease stage and lymphocytosis (Bojarska-Junak et al., 2008). Regardless, it is very difficult to know precise physiologic levels of secreted or membrane-bound TNFα in the *in vivo* BM HSPC niche and thus the relevance to *in vivo* or *in vitro* levels cannot be determined. Multiple studies have reported that CLL B cells constitutively produce TNFα *in vitro* in the 20pg/mL range that can be effectively neutralized by an anti-TNF antibody (Aue et al., 2011; Djurdjevic et al., 2009; Rosati et al., 2005). This is important as the levels of TNFα production *in vitro* are strikingly consistent with reported serum levels of TNFα in patients, which was validated in an independent study with a different cohort of CLL patients (Ferrajoli et al., 2002). An interesting, but potentially relevant, observation by another group was that cellular release of TNFα by primary CLL B cells was higher in early stage (Rai 0–1) compared with advanced stage (Rai II–III) patients, and the majority of CLL B cells used in our *in vitro* co-cultures were from early stage patients (Foa et al., 1990) (Table S1). Regardless, TNFα inhibits human CFU assays at a range of 1–10ng/mL (Skobin et al., 2000). We show that as little as 0.8μg of anti-TNF antibody mediated complete neutralization of the 25ng/mL exogenous TNFα added to our co-cultures (Figure S6), providing confidence that we are achieving complete TNFα neutralization of either recombinant or CLL-derived TNFα. Importantly, our heterogeneous CLL patient and donor input samples gave a striking uniformity of results, suggesting that the modulation of HSPCs is a shared feature of CLL cells. We also note that TNFα signaling promotes CLL B cell survival and that inhibition of that pathway could result in increased susceptibility to apoptosis (Cordingley et al., 1988; Digel et al., 1989; Durr et al., 2018). However, neutralization of TNFα in our short-term co-culture system did not change the viability of any cell fraction studied (CLL cells or HSPCs).

Resource availability

Lead contact

Further information and requests for resources and reagents should be directed to and will be fulfilled by the Lead Contact, Kay Medina (medina.kay@mayo.edu).

Materials availability

This study did not generate new unique reagents.

Data and code availability

This study did not generate or analyze datasets. Further, it did not produce any original code. The code for the R packages used in this manuscript can be found within the references provided.

Methods

All methods can be found in the accompanying Transparent methods supplemental file.

Supplemental information

Supplemental information can be found online at https://doi.org/10.1016/j.isci.2020.101994.

Acknowledgments

We thank Dr. Susan Slager for statistical advice and Susan Schwager for providing CLL patient data. The Mayo Clinic Department of Hematology specimen processing and the Predolin biobanking team provided many of the samples utilized in this study. We also thank Matthew Holets and the Mayo Clinic Charlton Clinical Research and Trials Unit for assisting with donor recruitment and sample collection. This study was supported by Mayo Clinic NIH Grant Relief funding to K.L.M. and NIH T32 funding (NIH T32 AI07425-23) awarded to B.A.M.

Author contributions

B.A.M., K.L.M., and N.E.K. wrote the manuscript. B.A.M., K.A.G., P.K.L., and B.M.W. performed and analyzed all experiments. J.E.K. provided expertise with the R program and assisted with UMAP generation. All authors reviewed and contributed to manuscript revisions.

Declaration of interests

Research funding to S.A.P. has been provided from Pharmacyclics, MorphoSys, Janssen, AstraZeneca, TG Therapeutics, Celgene, AbbVie, and Ascentage Pharma for clinical studies in which S.A.P. is a principal investigator. S.A.P. also participated in Advisory Board meetings of Pharmacyclics, AstraZeneca, Genentech, Gilead, GlaxoSmithKline, Verastem Oncology, and AbbVie (he was not personally compensated for his participation). Research funding to N.E.K. has been provided from Acerta Pharma BV, Celgene, Genentech, Pharmacyclics, and Tolero Pharmaceutical. N.E.K. also participates in the data safety monitoring committees of Agios Pharm, Astra Zeneca, Celgene, Cytomx Therapeutics, Genentech, Infinity Pharm, Morpho-Sys, and Pharmacyclics (he was not personally compensated for his participation). All other authors declare no competing interests.

Received: July 22, 2020
Revised: November 15, 2020
Accepted: December 22, 2020
Published: January 22, 2021

References

Arinobu, Y., Mizuno, S., Chong, Y., Shigematsu, H., Iino, T., Iwasaki, H., Graf, T., Mayfield, R., Chan, S., Kastner, P., et al. (2007). Reciprocal activation of GATA-1 and PU.1 marks initial specification of hematopoietic stem cells into myeloerythroid and myelolymphoid lineages. Cell Stem Cell *1*, 416–427.

Aue, G., Nelson Lozier, J., Tian, X., Cullinane, A.M., Soto, S., Samsel, L., McCoy, P., and Wiestner, A. (2011). Inflammation, TNFalpha and endothelial dysfunction link lenalidomide to venous thrombosis in chronic lymphocytic leukemia. Am. J. Hematol. *86*, 835–840.

Bojarska-Junak, A., Hus, I., Szczepanek, E.W., Dmoszynska, A., and Rolinski, J. (2008). Peripheral blood and bone marrow TNF and TNF receptors in early and advanced stages of B-CLL in correlation with ZAP-70 protein and CD38 antigen. Leuk. Res. *32*, 225–233.

Bresnick, E.H., Katsumura, K.R., Lee, H.Y., Johnson, K.D., and Perkins, A.S. (2012). Master regulatory GATA transcription factors: mechanistic principles and emerging links to hematologic malignancies. Nucleic Acids Res. *40*, 5819–5831.

Broxmeyer, H.E., Williams, D.E., Lu, L., Cooper, S., Anderson, S.L., Beyer, G.S., Hoffman, R., and Rubin, B.Y. (1986). The suppressive influences of human tumor necrosis factors on bone marrow hematopoietic progenitor cells from normal donors and patients with leukemia: synergism of tumor necrosis factor and interferon-gamma. J. Immunol. *136*, 4487–4495.

Buck, I., Morceau, F., Cristofanon, S., Reuter, S., Dicato, M., and Diederich, M. (2009). The inhibitory effect of the proinflammatory cytokine TNFalpha on erythroid differentiation involves erythroid transcription factor modulation. Int. J. Oncol. *34*, 853–860.

Burda, P., Laslo, P., and Stopka, T. (2010). The role of PU.1 and GATA-1 transcription factors during normal and leukemogenic hematopoiesis. Leukemia *24*, 1249–1257.

Burger, J.A., Quiroga, M.P., Hartmann, E., Bürkle, A., Wierda, W.G., Keating, M.J., and Rosenwald, A. (2009). High-level expression of the T-cell chemokines CCL3 and CCL4 by chronic lymphocytic leukemia B cells in nurselike cell cocultures and after BCR stimulation. Blood *113*, 3050.

Cordingley, F.T., Hoffbrand, A.V., Heslop, H.E., Turner, M., Bianchi, A., Reittie, J.E., Vyakarnam, A., Meager, A., and Brenner, M.K. (1988). Tumour necrosis factor as an autocrine tumour growth factor for chronic B-cell malignancies. Lancet *331*, 969–971.

Digel, W., Stefanic, M., Schoniger, W., Buck, C., Raghavachar, A., Frickhofen, N., Heimpel, H., and Porzsolt, F. (1989). Tumor necrosis factor induces proliferation of neoplastic B cells from chronic lymphocytic leukemia. Blood *73*, 1242–1246.

DiLillo, D.J., Weinberg, J.B., Yoshizaki, A., Horikawa, M., Bryant, J.M., Iwata, Y., Matsushita, T., Matta, K.M., Chen, Y., Venturi, G.M., et al. (2013). Chronic lymphocytic leukemia and regulatory B cells share IL-10 competence and immunosuppressive function. Leukemia *27*, 170–182.

Djurdjevic, P., Zelen, I., Ristic, P., Baskic, D., Popovic, S., and Arsenijevic, N. (2009). Role of decreased production of interleukin-10 and interferon-gamma in spontaneous apoptosis of B-chronic lymphocytic leukemia lymphocytes in vitro. Arch. Med. Res. *40*, 357–363.

Doulatov, S., Notta, F., Laurenti, E., and Dick, J.E. (2012). Hematopoiesis: a human perspective. Cell Stem Cell *10*, 120–136.

Durr, C., Hanna, B.S., Schulz, A., Lucas, F., Zucknick, M., Benner, A., Clear, A., Ohl, S., Ozturk, S., Zenz, T., et al. (2018). Tumor necrosis factor receptor signaling is a driver of chronic lymphocytic leukemia that can be therapeutically targeted by the flavonoid wogonin. Haematologica *103*, 688–697.

Dybedal, I., Bryder, D., Fossum, A., Rusten, L.S., and Jacobsen, S.E. (2001). Tumor necrosis factor (TNF)-mediated activation of the p55 TNF receptor negatively regulates maintenance of cycling reconstituting human hematopoietic stem cells. Blood *98*, 1782–1791.

Etzrodt, M., Ahmed, N., Hoppe, P.S., Loeffler, D., Skylaki, S., Hilsenbeck, O., Kokkaliaris, K.D., Kaltenbach, H.M., Stelling, J., Nerlov, C., et al. (2019). Inflammatory signals directly instruct PU.1 in HSCs via TNF. Blood *133*, 816–819.

Fayad, L., Keating, M.J., Reuben, J.M., O'Brien, S., Lee, B.N., Lerner, S., and Kurzrock, R. (2001). Interleukin-6 and interleukin-10 levels in chronic lymphocytic leukemia: correlation with phenotypic characteristics and outcome. Blood *97*, 256–263.

Fecteau, J.F., and Kipps, T.J. (2012). Structure and function of the hematopoietic cancer niche: focus on chronic lymphocytic leukemia. Front. Biosci. (Schol Ed. *4*, 61–73.

Ferrajoli, A., Keating, M.J., Manshouri, T., Giles, F.J., Dey, A., Estrov, Z., Koller, C.A., Kurzrock, R., Thomas, D.A., Faderl, S., et al. (2002). The clinical significance of tumor necrosis factor-alpha plasma level in patients having chronic lymphocytic leukemia. Blood *100*, 1215–1219.

Foa, R., Massaia, M., Cardona, S., Tos, A.G., Bianchi, A., Attisano, C., Guarini, A., di Celle, P.F., and Fierro, M.T. (1990). Production of tumor necrosis factor-alpha by B-cell chronic lymphocytic leukemia cells: a possible regulatory role of TNF in the progression of the disease. Blood *76*, 393–400.

Forconi, F., and Moss, P. (2015). Perturbation of the normal immune system in patients with CLL. Blood *126*, 573–581.

Geissler, R.G., Ottmann, O.G., Eder, M., Kojouharoff, G., Hoelzer, D., and Ganser, A. (1991). Effect of recombinant human transforming growth factor beta and tumor necrosis factor alpha on bone marrow progenitor cells of HIV-infected persons. Ann. Hematol. *62*, 151–155.

Goldman, D. (2000). Chronic lymphocytic leukemia and its impact on the immune system. Clin. J. Oncol. Nurs. *4*, 233–234, 236.

Grell, M., Douni, E., Wajant, H., Löhden, M., Clauss, M., Maxeiner, B., Georgopoulos, S., Lesslauer, W., Kollias, G., Pfizenmaier, K., et al. (1995). The transmembrane form of tumor necrosis factor is the prime activating ligand of the 80 kDa tumor necrosis factor receptor. Cell *83*, 793–802.

Grigorakaki, C., Morceau, F., Chateauvieux, S., Dicato, M., and Diederich, M. (2011). Tumor necrosis factor alpha-mediated inhibition of erythropoiesis involves GATA-1/GATA-2 balance impairment and PU.1 over-expression. Biochem. Pharmacol. *82*, 156–166.

Hu, Y., and Smyth, G.K. (2009). ELDA: extreme limiting dilution analysis for comparing depleted and enriched populations in stem cell and other assays. J. Immunol. Methods *347*, 70–78.

Janel, A., Dubois-Galopin, F., Bourgne, C., Berger, J., Tarte, K., Boiret-Dupre, N., Boisgard, S., Verrelle, P., Dechelotte, P., Tournilhac, O., et al. (2014). The chronic lymphocytic leukemia clone disrupts the bone marrow microenvironment. Stem Cells Dev. *23*, 2972–2982.

Kang, Y.J., Yang, S.J., Park, G., Cho, B., Min, C.K., Kim, T.Y., Lee, J.S., and Oh, I.H. (2007). A novel function of interleukin-10 promoting self-renewal of hematopoietic stem cells. Stem Cells *25*, 1814–1822.

Kay, N.E., Bone, N.D., Tschumper, R.C., Howell, K.H., Geyer, S.M., Dewald, G.W., Hanson, C.A., and Jelinek, D.F. (2002). B-CLL cells are capable of synthesis and secretion of both pro- and anti-angiogenic molecules. Leukemia *16*, 911.

Kim, M., Pyo, S., Kang, C.H., Lee, C.O., Lee, H.K., Choi, S.U., and Park, C.H. (2018). Folate receptor 1 (FOLR1) targeted chimeric antigen receptor (CAR) T cells for the treatment of gastric cancer. PLoS One *13*, e0198347.

Kipps, T.J., Stevenson, F.K., Wu, C.J., Croce, C.M., Packham, G., Wierda, W.G., O'Brien, S., Gribben, J., and Rai, K. (2017). Chronic lymphocytic leukaemia. Nat. Rev. Dis. Primers *3*, 17008.

Lagneaux, L., Delforge, A., Dorval, C., Bron, D., and Stryckmans, P. (1993). Excessive production of transforming growth factor-beta by bone marrow stromal cells in B-cell chronic lymphocytic leukemia inhibits growth of hematopoietic precursors and interleukin-6 production. Blood *82*, 2379–2385.

Lahat, N., Aghai, E., Maroun, B., Kinarty, A., Quitt, M., and Froom, P. (1991). Increased spontaneous secretion of IL-6 from B cells of patients with B chronic lymphatic leukaemia (B-CLL) and autoimmunity. Clin. Exp. Immunol. *85*, 302–306.

Leland McInnes, J.H. (2018). UMAP: uniform manifold approximation and projection for dimension reduction. https://arxivorg/abs/180203426.

Liu, M., Miller, C.L., and Eaves, C.J. (2013). Human long-term culture initiating cell assay. Methods Mol. Biol. *946*, 241–256.

Liu, T., Zhang, L., Joo, D., and Sun, S.C. (2017). NF-kappaB signaling in inflammation. Signal Transduct. Target. Ther. *2*, 17023.

Lotz, M., Ranheim, E., and Kipps, T.J. (1994). Transforming growth factor beta as endogenous growth inhibitor of chronic lymphocytic leukemia B cells. J. Exp. Med. *179*, 999.

Maguer-Satta, V., Oostendorp, R., Reid, D., and Eaves, C.J. (2000). Evidence that ceramide mediates the ability of tumor necrosis factor to modulate primitive human hematopoietic cell fates. Blood *96*, 4118–4123.

Manso, B.A., Zhang, H., Mikkelson, M.G., Gwin, K.A., Secreto, C.R., Ding, W., Parikh, S.A., Kay, N.E., and Medina, K.L. (2019). Bone marrow hematopoietic dysfunction in untreated chronic lymphocytic leukemia patients. Leukemia *33*, 638–652.

Means, R.T., Jr., Dessypris, E.N., and Krantz, S.B. (1990). Inhibition of human colony-forming-unit erythroid by tumor necrosis factor requires accessory cells. J. Clin. Invest. *86*, 538–541.

Michalevicz, R., Porat, R., Vechoropoulos, M., Baron, S., Yanoov, M., Cycowitz, Z., and Shibolet, S. (1991). Restoration of in vitro hematopoiesis in B-chronic lymphocytic leukemia by antibodies to tumor necrosis factor. Leuk. Res. *15*, 111–120.

Moriguchi, T., and Yamamoto, M. (2014). A regulatory network governing Gata1 and Gata2 gene transcription orchestrates erythroid lineage differentiation. Int. J. Hematol. *100*, 417–424.

Nakagawa, M.M., Chen, H., and Rathinam, C.V. (2018). Constitutive activation of NF-kappaB pathway in hematopoietic stem cells causes loss of quiescence and deregulated transcription factor networks. Front. Cell Dev. Biol. *6*, 143.

Novershtern, N., Subramanian, A., Lawton, L.N., Mak, R.H., Haining, W.N., McConkey, M.E., Habib, N., Yosef, N., Chang, C.Y., Shay, T., et al. (2011). Densely interconnected transcriptional circuits control cell states in human hematopoiesis. Cell *144*, 296–309.

Pang, W.W., Schrier, S.L., and Weissman, I.L. (2017). Age-associated changes in human

hematopoietic stem cells. Semin. Hematol. *54*, 39–42.

Petzer, A.L., Zandstra, P.W., Piret, J.M., and Eaves, C.J. (1996). Differential cytokine effects on primitive (CD34+CD38-) human hematopoietic cells: novel responses to Flt3-ligand and thrombopoietin. J. Exp. Med. *183*, 2551–2558.

Pronk, C.J., Veiby, O.P., Bryder, D., and Jacobsen, S.E. (2011). Tumor necrosis factor restricts hematopoietic stem cell activity in mice: involvement of two distinct receptors. J. Exp. Med. *208*, 1563–1570.

Rosati, E., Sabatini, R., Tabilio, A., Di Ianni, M., Bartoli, A., and Marconi, P. (2005). B-chronic lymphocytic leukemia cells exert an in vitro cytotoxicity mediated by tumor necrosis factor alpha. Leuk. Res. *29*, 829–839.

Rothhammer, V., Borucki, D.M., Kenison, J.E., Hewson, P., Wang, Z., Bakshi, R., Sherr, D.H., and Quintana, F.J. (2018). Detection of aryl hydrocarbon receptor agonists in human samples. Sci. Rep. *8*, 4970.

Sala, R., Mauro, F.R., Bellucci, R., De Propris, M.S., Cordone, I., Lisci, A., Foa, R., and de Fabritiis, P. (1998). Evaluation of marrow and blood haemopoietic progenitors in chronic lymphocytic leukaemia before and after chemotherapy. Eur. J. Haematol. *61*, 14–20.

Saulep-Easton, D., Vincent, F.B., Quah, P.S., Wei, A., Ting, S.B., Croce, C.M., Tam, C., and Mackay, F. (2016). The BAFF receptor TACI controls IL-10 production by regulatory B cells and CLL B cells. Leukemia *30*, 163–172.

Skobin, V., Jelkmann, W., Morschakova, E., Pavlov, A.D., and Schlenke, P. (2000). Tumor necrosis factor-alpha and TNF-beta inhibit clonogenicity of mobilized human hematopoietic progenitors. J. Interferon Cytokine Res. *20*, 507–510.

Tian, T., Wang, M., and Ma, D. (2014). TNF-alpha, a good or bad factor in hematological diseases? Stem Cell Investig *1*, 12.

Tsopra, O.A., Ziros, P.G., Lagadinou, E.D., Symeonidis, A., Kouraklis-Symeonidis, A., Thanopoulou, E., Angelopoulou, M.K., Vassilakopoulos, T.P., Pangalis, G.A., and Zoumbos, N.C. (2009). Disease-related anemia in chronic lymphocytic leukemia is not due to intrinsic defects of erythroid precursors: a possible pathogenetic role for tumor necrosis factor-alpha. Acta Haematol. *121*, 187–195.

van Attekum, M.H., Eldering, E., and Kater, A.P. (2017). Chronic lymphocytic leukemia cells are active participants in microenvironmental cross-talk. Haematologica *102*, 1469–1476.

Vicente, C., Conchillo, A., Garcia-Sanchez, M.A., and Odero, M.D. (2012). The role of the GATA2 transcription factor in normal and malignant hematopoiesis. Crit. Rev. Oncol. Hematol. *82*, 1–17.

Walsh, J.C., DeKoter, R.P., Lee, H.J., Smith, E.D., Lancki, D.W., Gurish, M.F., Friend, D.S., Stevens, R.L., Anastasi, J., and Singh, H. (2002). Cooperative and antagonistic interplay between PU.1 and GATA-2 in the specification of myeloid cell fates. Immunity *17*, 665–676.

Wang, W., Fujii, H., Kim, H.J., Hermans, K., Usenko, T., Xie, S., Luo, Z.J., Ma, J., Celso, C.L., Dick, J.E., et al. (2017). Enhanced human hematopoietic stem and progenitor cell engraftment by blocking donor T cell-mediated TNFalpha signaling. Sci. Transl. Med. *9*, eaag3214.

Wolff, L., and Humeniuk, R. (2013). Concise review: erythroid versus myeloid lineage commitment: regulating the master regulators. Stem Cells *31*, 1237–1244.

Zent, C.S., Ding, W., Schwager, S.M., Reinalda, M.S., Hoyer, J.D., Jelinek, D.F., Tschumper, R.C., Bowen, D.A., Call, T.G., Shanafelt, T.D., et al. (2008). The prognostic significance of cytopenia in chronic lymphocytic leukaemia/small lymphocytic lymphoma. Br. J. Haematol. *141*, 615–621.

Zhang, P., Zhang, X., Iwama, A., Yu, C., Smith, K.A., Mueller, B.U., Narravula, S., Torbett, B.E., Orkin, S.H., and Tenen, D.G. (2000). PU.1 inhibits GATA-1 function and erythroid differentiation by blocking GATA-1 DNA binding. Blood *96*, 2641–2648.

iScience, Volume *24*

Supplemental Information

Chronic lymphocytic leukemia B-cell-derived TNFα impairs bone marrow myelopoiesis

Bryce A. Manso, Jordan E. Krull, Kimberly A. Gwin, Petra K. Lothert, Baustin M. Welch, Anne J. Novak, Sameer A. Parikh, Neil E. Kay, and Kay L. Medina

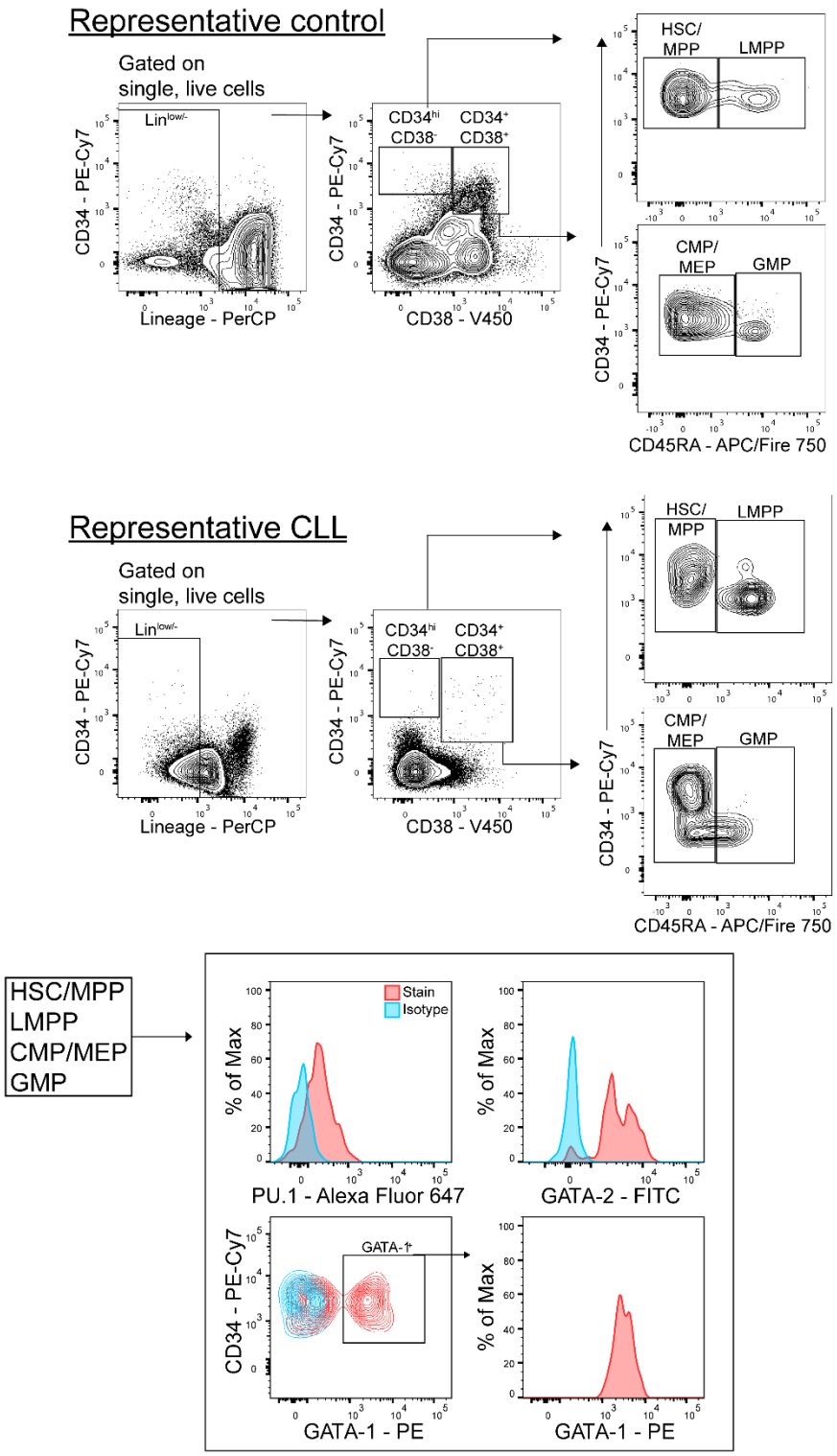

Figure S1. Flow cytometry gating strategy for *ex vivo* and *in vitro* HSPCs and transcription factors. Related to Figures 1-3. The sequential gating strategy used for analysis is illustrated using representative control and CLL *ex vivo* bone marrow samples. Following gating, each population was assessed for expression of PU.1, GATA-2, and GATA-1 as shown.

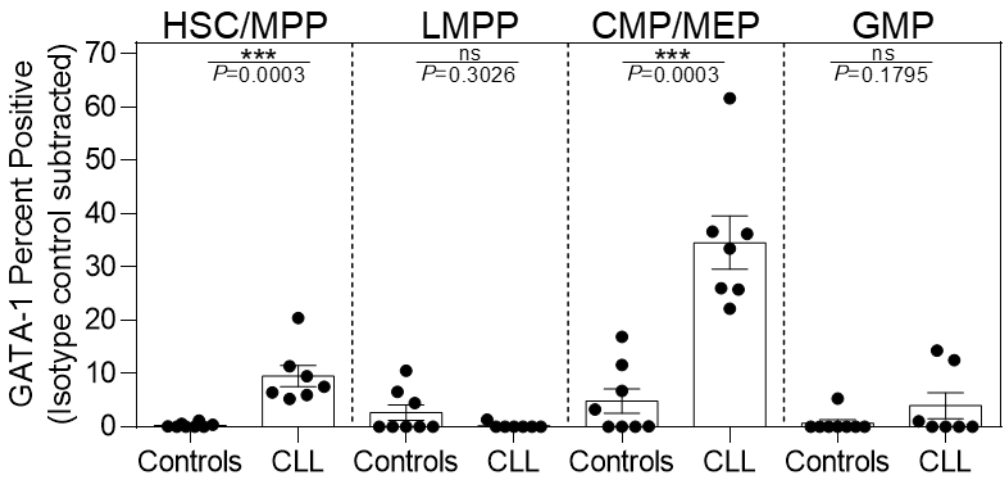

Figure S2. Frequency of GATA-1^{+} cells among HSPCs from control and CLL patient bone marrow. Related to Figure 1. Freshly isolated BM was evaluated by intranuclear flow cytometry for the frequency of GATA-1 positive cells among HSC/MPP, LMPP, CMP/MEP, and GMP populations. Each point represents individual donors and Data is presented as mean +/- SEM. Control n=8 and CLL n=7. ***P<0.001 and ns by Mann-Whitney U test.

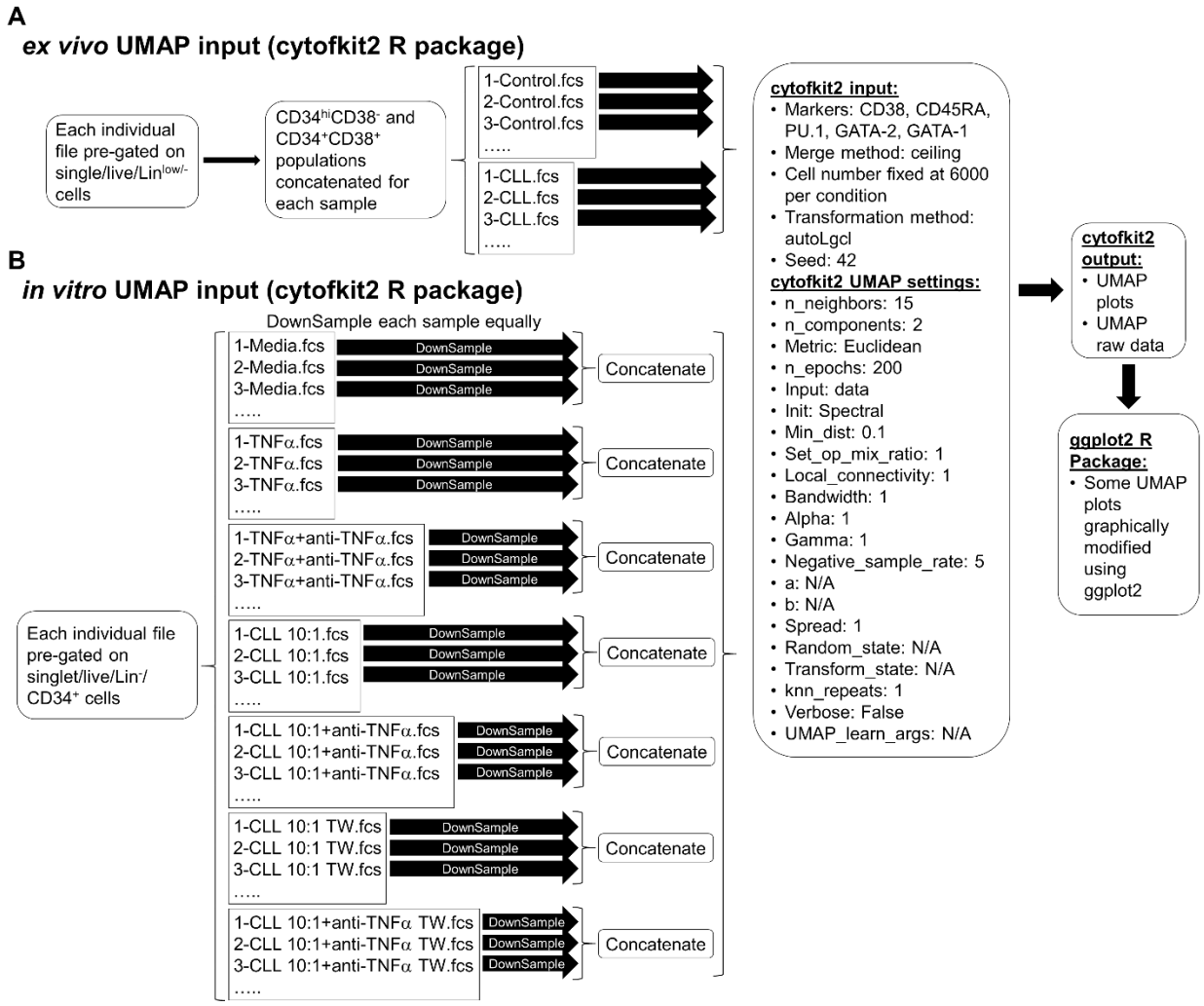

Figure S3. Experimental design and input for *ex vivo* and *in vitro* UMAP analysis. Related to Figures 1 and 4. (**A**) $CD34^{hi}CD38^{-}$ and $CD34^{+}CD38^{+}$ populations among the $Lin^{low/-}$ compartment were concatenated in FlowJo and used as the raw data input for the *ex vivo* UMAP analysis. Data from the *ex vivo* flow cytometry analysis was exported from FlowJo and imported directly into the cytofkit2 R package with the settings and pipeline outlined. (**B**) $Lin^{-}CD34^{+}$ cells were used as the raw data input for the *in vitro* UMAP analysis. Each individual *in vitro* data file was pre-processed in FlowJo by using the DownSample plugin to obtain files of 1000 $Lin^{-}CD34^{+}$ cells. All data files from each individual *in vitro* condition was then concatenated and DownSampled to 6000 total cells prior to inputting into R using the cytofkit2 package and pipeline outlined. All UMAP graphical plots and raw data was generated and the raw UMAP data was further graphed using the ggplot2 R package or inputting the analyzed data back into FlowJo. Each UMAP figure is indicative of the combination (or specific subsets) of the total *ex vivo* or *in vitro* data.

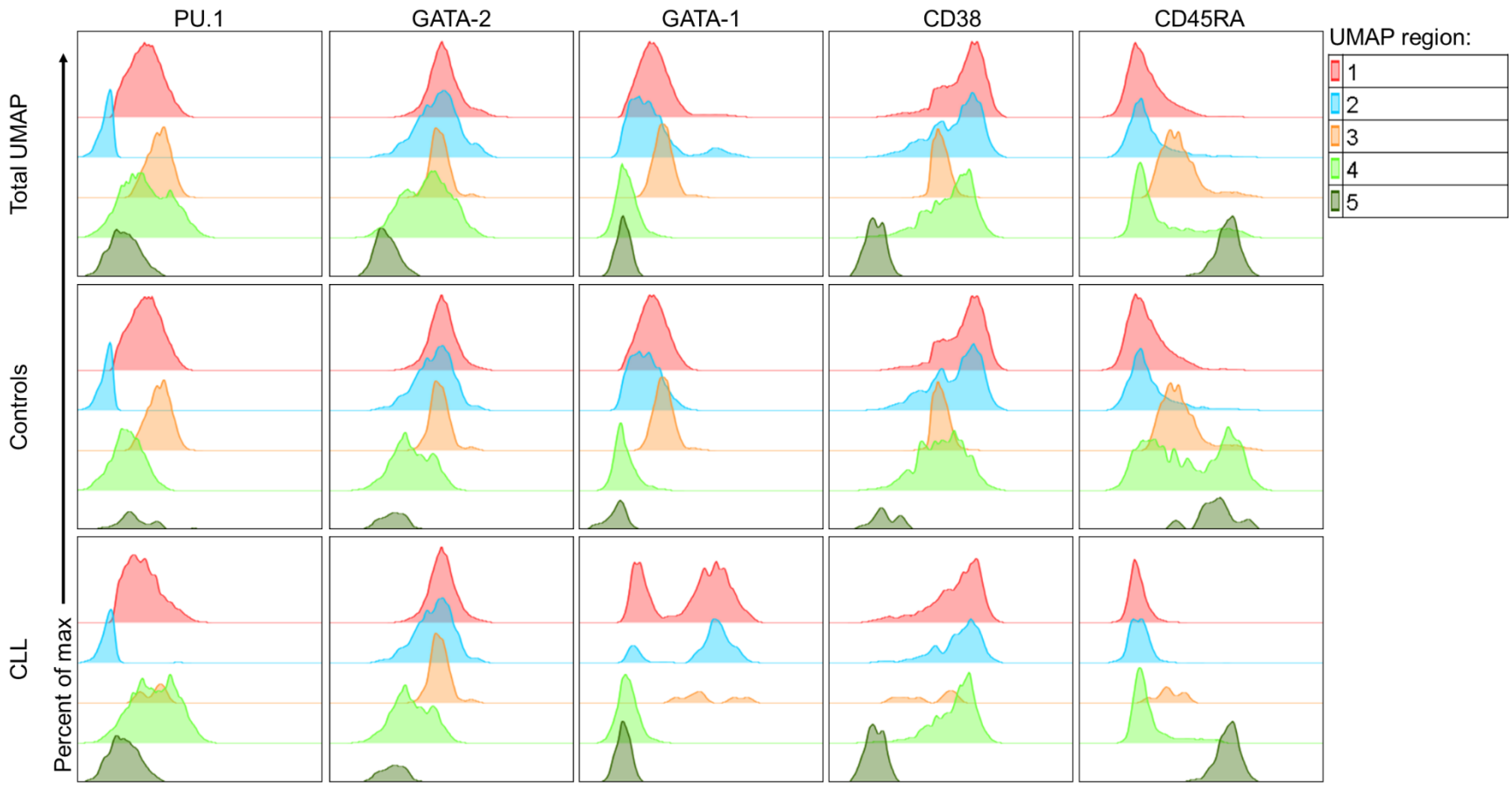

Figure S4. *ex vivo* UMAP marker expression patterns. Related to Figure 1. The analyzed *ex vivo* UMAP data from the cytofkit2 R package was imported back into FlowJo for further analysis. Each of the five individual regions were overlaid for the expression of the clustering markers. Each histogram represents the normalized expression data for each marker as calculated during the UMAP analysis. The histogram overlays are displayed as either the total UMAP (controls and CLL) or cells from the control or CLL cohorts only.

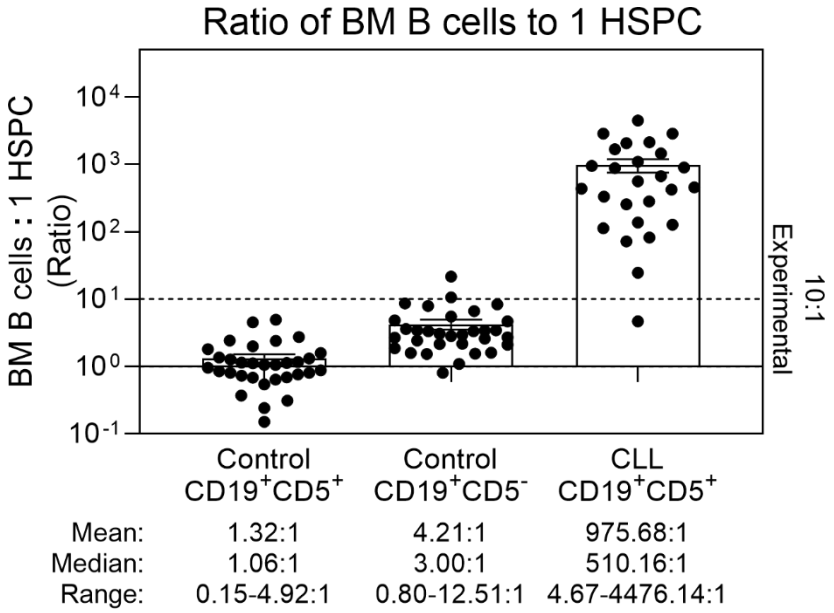

Figure S5. Determination of the *ex vivo* bone marrow B cell:HSPC BM ratio. Related to Figures 2-4. Freshly isolated control (n=32) or CLL (n=26) BM was analyzed by flow cytometry to determine the frequency of $CD19^+CD5^+$ and $CD19^+CD5^-$ B cells and Lin^-CD34^+ HSPCs among total BM cells. This data was generated from our previously published data set(Manso et al., 2019). The ratio for each individual sample (represented by a single point) was determined by dividing the frequency of either $CD19^+CD5^+$ or $CD19^+CD5^-$ B cells by the frequency Lin^-CD34^+ HSPCs. Data is presented as the mean +/- SEM.

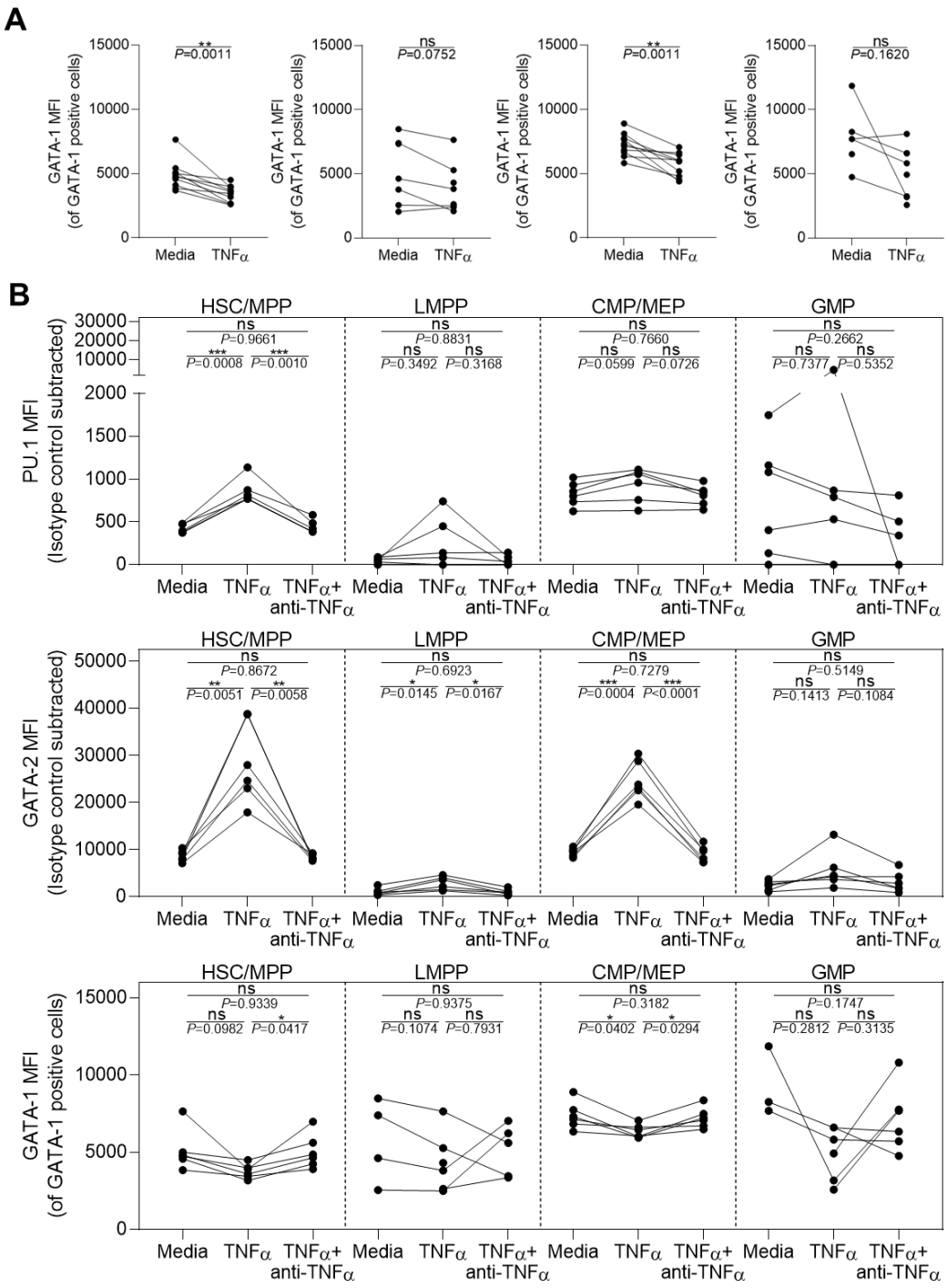

Figure S6. Effect of TNFα on transcription factor expression in HSPCs. Related to Figures 3 and 4. (**A**) Freshly isolated control Lin$^-$CD34$^+$ HSPCs were exposed to TNFα as described in the Transparent Methods (n=10 or 6). Following 24 hours of culture, intranuclear flow cytometry was performed to determine the expression of GATA-1. ***P*<0.01 and ns by paired t-test. (**B**) Additional cultures were set up as in (A) and received a neutralizing antibody against TNFα (anti-TNFα) at the start of the experiment (n=6). Following 24 hours of culture, intranuclear flow cytometry was performed to determine the expression of PU.1, GATA-2, and GATA-1. Each point represents an individual donor with lines connecting the same donor across different experimental conditions. **P*<0.05, ***P*<0.01, ****P*<0.001, and ns by repeated measures one-way ANOVA adjusted for multiple comparisons.

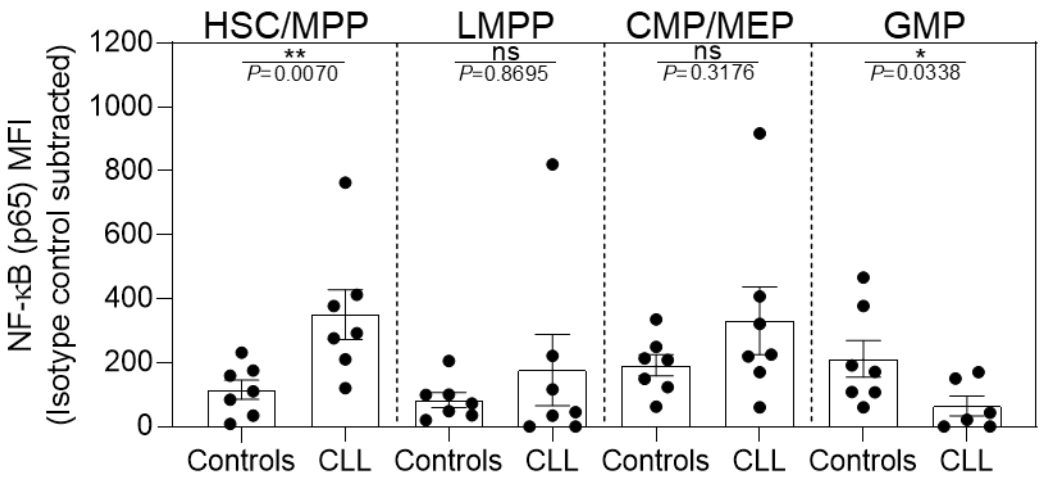

Figure S7. *ex vivo* analysis of NF-κB. Related to Figure 1. Freshly prepared BM from control and CLL patients were evaluated by intranuclear flow cytometry for expression of NF-κB p65 among HSC/MPPs, LMPP, CMP/MEPs, and GMPs. Each point represents individual donors and Data is presented as mean +/- SEM. Control n=7 and CLL n=7. *P<0.05, **P<0.01, and ns by Mann-Whitney U test.

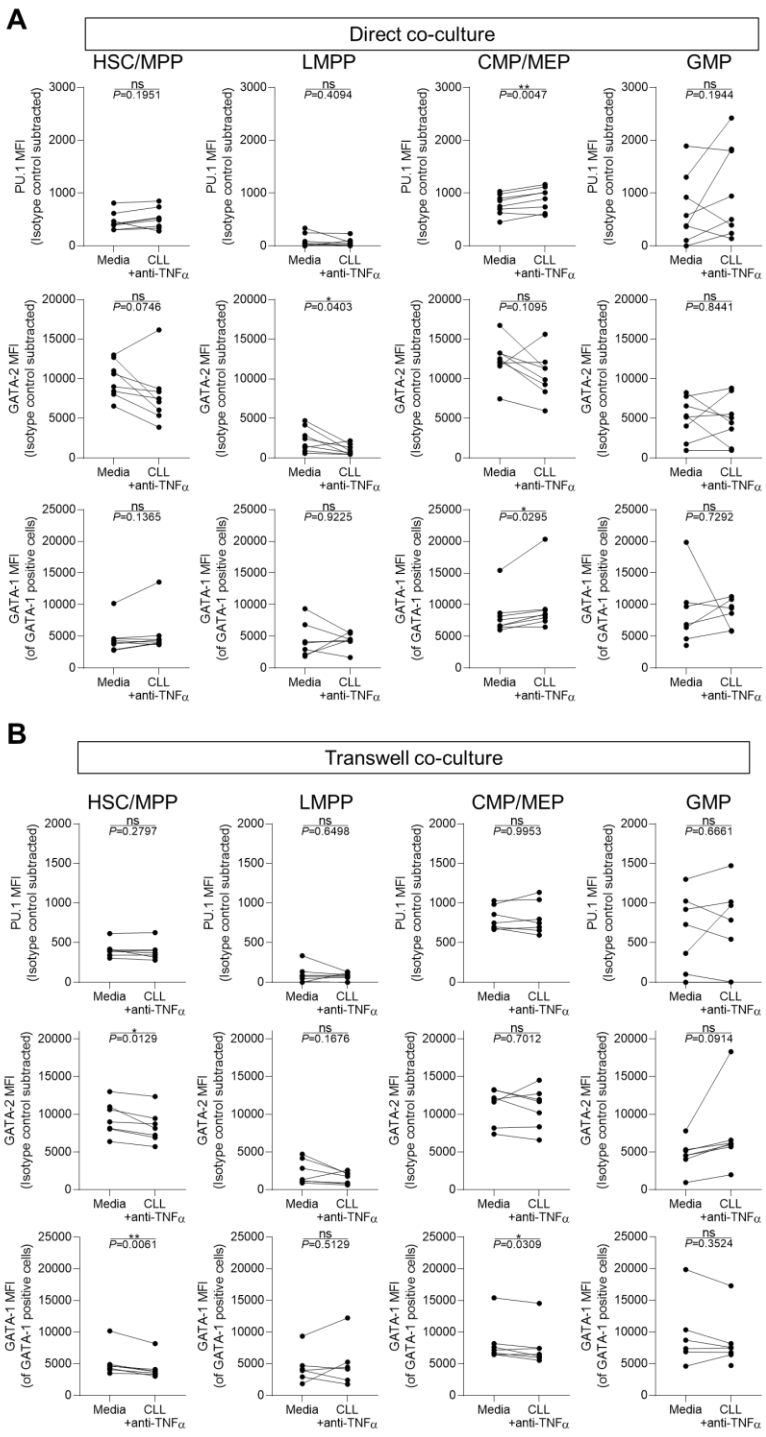

Figure S8. Neutralization of TNFα normalizes transcription factor expression in CLL:HSPC co-cultures. Related to Figures 2-4. The HSC/MPP, LMPP, CMP/MEP, and GMP subsets were evaluated by flow cytometry for relative levels of PU.1, GATA-2, and GATA-1 protein levels (by MFI) between media controls and CLL+anti-TNFα cultures. All CLL co-cultures at a ratio of 10:1 (CLL cells:HSPCs). Evaluation of direct (**A**) and 1.0μm Transwell (**B**) co-cultures was performed. Each point and connecting line represents a unique pairing of a control HSPC donor and CLL patient (n=11 for direct co-culture and n=7 for TW co-cultures, 11 individual experiments). *P<0.05, **P<0.01, and ns by paired t-test.

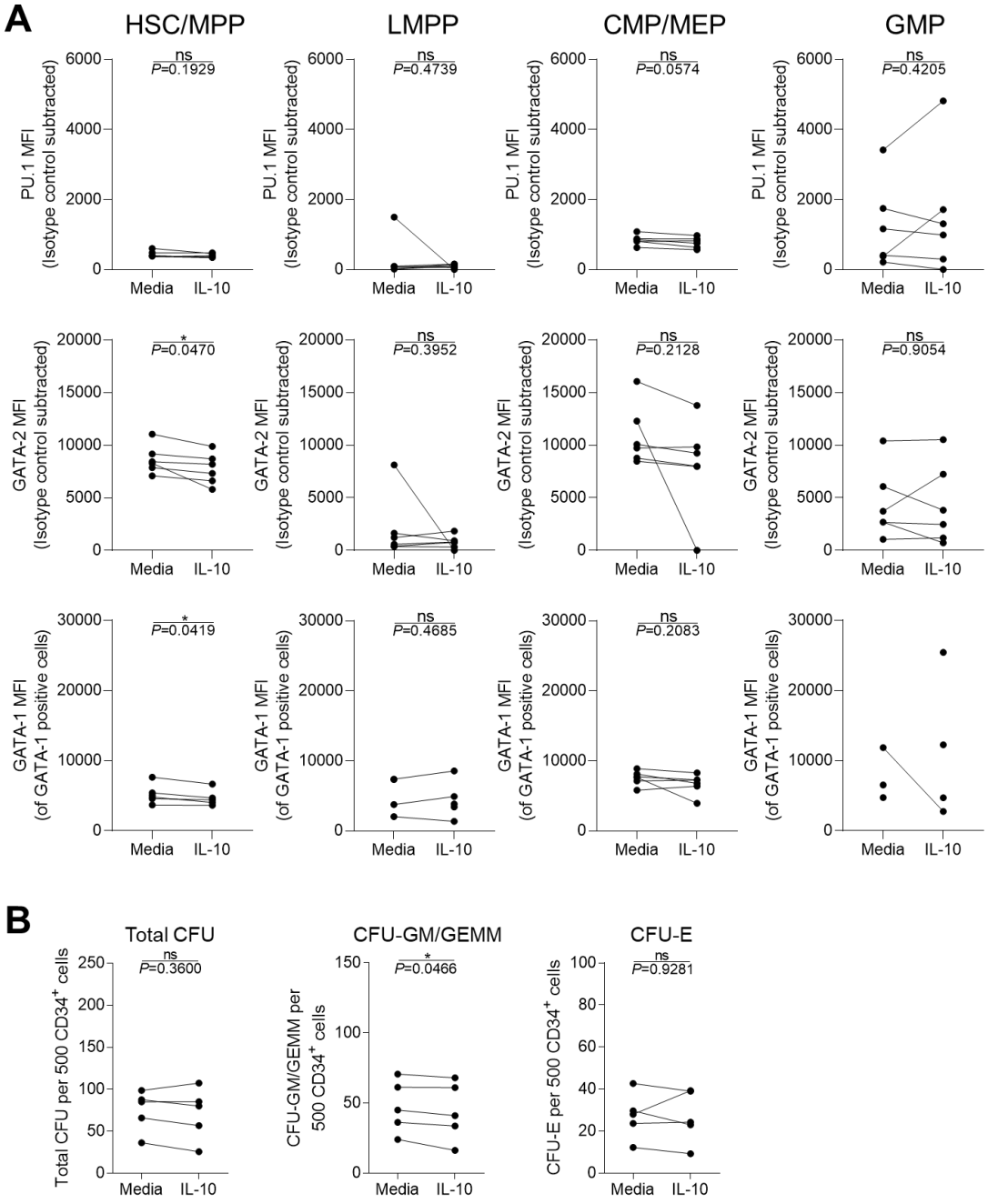

Figure S9. IL-10 does not alter levels of PU.1, GATA-2, or GATA-1 in HSPCs or change colony forming unit (CFU) capacity. Related to Figures 2-4. (**A**) Freshly isolated control CD34$^+$ HSPCs from BM were exposed *in vitro* to IL-10 for 24 hours. Following incubation, the HSPCs were analyzed by intranuclear flow cytometry for expression of PU.1, GATA-2, and GATA-1 as described in the Transparent Methods. Each point and connected line represents a unique donor (n=6). Some culture conditions did not contain detectable GATA-1 protein among GMPs and therefore are not represented in the graph. (**B**) Freshly isolated CD34$^+$ HSPCs from control BM were plated in triplicate CFU assays. CFU assays were supplemented at assay initiation with 25 ng/mL IL-10 (n=5). Each point and connected line represents a unique donor. *P<0.05 and ns by paired t-test.

												Experimental use of samples:			
CLL ID	**Age**	**Sex**	**Rai Stage**	**Cytogenetics**	**ZAP-70**	**CD38**	**CD49d**	**B2M**	**IGHV**	**Leukemic marrow involvement (%) – hematopathology**	**Sample tissue type**	***ex vivo* TFs**	***ex vivo* UMAP**	***in vitro* co-culture**	**LTC-IC assay**
CLL-1	66	M	0	Trisomy 12	+	-	+	+	UM	>90	BM	X			
CLL-2	68	F	I	13q-	-	-	-	+	M	10	BM	X			X
CLL-3	80	M	II	Trisomy 12	+	-	+	+	UM	90	BM	X			X
CLL-4	68	M	I	11q-	-	-	n.d.	+	UM	90	BM	X			X
CLL-5	58	M	I	13q-	+	-	-	+	UM	90	BM	X			X
CLL-6	58	F	III	Trisomy 12	+	-	n.d.	+	UM	80	BM	X			X
CLL-7	75	F	0	13q-	-	-	n.d.	+	UM	80	BM	X	X		
CLL-8	79	F	II	Trisomy 12	-	-	+	+	M	30	BM	X	X		
CLL-9	40	M	II	Trisomy 12	n.d.	+	n.d.	+	M	n.d.	BM	X	X		
CLL-10	63	F	III	13q-	+	-	+	+	UM	90	BM	X	X		
CLL-11	58	M	II	Trisomy 12	-	+	+	+	M	90	BM	X	X		
CLL-12	63	M	IV	13q-	+	+	+	+	UM	95	BM	X	X		X
CLL-13	53	M	0	13q-	+	-	-	+	UM	n.d.	BM	X	X		X
CLL-14	71	M	IV	Normal	-	-	+	+	M	<1	BM				X
CLL-15	56	M	0	17p-	+	+	-	+	UM	80	BM				X
CLL-16	41	M	I	Normal	+	-	+	+	M	20	BM	X	X		
CLL-17	74	M	0	13q-	-	-	-	-	M	n.d.	Blood			X	
CLL-18	67	M	0	Normal	-	-	-	-	M	n.d.	Blood			X	
CLL-19	69	F	III	13q-	-	-	-	+	M	90	Blood			X	
CLL-20	67	M	0	13q-	-	-		+	M	n.d.	Blood			X	
CLL-21	55	F	I	13q-	-	-	-	+	M	n.d.	Blood			X	
CLL-22	44	M	I	NA	-	-	-	+	UM	n.d.	Blood			X	
CLL-23	80	M	0	n.d.	-	-	-	+	M	n.d.	Blood			X	
CLL-24	71	M	0	Trisomy 12	+	-	+	+	UM	80	Blood			X	
CLL-25	92	F	0	13q-	-	-	-	+	M	n.d.	Blood			X	
CLL-26	80	M	0	Normal	-	-	-	+	M	n.d.	Blood			X	
CLL-27	82	M	0	Trisomy 12	-	+	-	+	UM	n.d.	Blood			X	

Table S1. CLL patient characteristics. Related to Figures 1-5. Demographics for each CLL patient are listed and the tissue source and list of experiments the sample was used for is indicated. B2M=beta 2 microglobulin, IGHV=immunoglobulin heavy chain variable region, M=mutated, UM=unmutated, +=positive, -=negative, BM = bone marrow, TF = transcription factor, and n.d.=no data.

Reagent or antibody specificity	Fluorochrome	Vendor	Catalogue Number	Clone	
Sample preparation reagents					
1X phosphate buffered saline (PBS) prepared from 10X stock	N/A	Gibco	14200-075	N/A	
Human Fc block	N/A	Miltenyi Biotec	130-059-901	N/A	
1% paraformaldehyde (PFA) prepared from 10% stock	N/A	Electron Microscopy Sciences	15712-S	N/A	
Cell culture reagents					
CellGenix GMP SCGM media	N/A	CellGenix	20802	N/A	
Recombinant human stem cell factor	N/A	PeproTech	300-07	N/A	
Recombinant human IL-6	N/A	PeproTech	200-06	N/A	
Recombinant human IL-3	N/A	PeproTech	200-03	N/A	
Recombinant human Erythropoietin	N/A	PeproTech	100-64	N/A	
Recombinant human TNFα	N/A	PeproTech	300-01A	N/A	
anti-human TNFα	N/A	R&D Systems	AF-210-NA	N/A	
Recombinant human IL-10	N/A	BioLegend	573202	N/A	
1.0 μm TransWell insert/plate	N/A	Corning	CLS3380	N/A	
MethoCult H4435 media	N/A	StemCell Technologies	04435	N/A	
MyeloCult H5100 media	N/A	StemCell Technologies	05150	N/A	
Hydrocortisone	N/A	StemCell Technologies	07904	N/A	
Cell Surface Markers					
Fixable Viability Stain 510	V510	BD Biosciences	564406	N/A	
CD3	PerCP	BD Biosciences	347344	Sk7	Lineage antibodies/ cocktail
CD5	PerCP	BioLegend	300618	UCHT2	
CD11b	PerCP	BioLegend	101230	M1/70	
CD14	PerCP	BD Biosciences	340660	MφP9	
CD19	PerCP	BD Biosciences	347544	4G7	
CD56	PerCP	BioLegend	318342	HCD56	
CD34	PE-Cy7	BD Biosciences	348791	8G12	
CD38	V450	BD Biosciences	646851	HB7	
CD45RA	APC/Fire 750	BioLegend	304152	HI100	
CD19	APC/Fire 750	BioLegend	363030	SJ25C1	
CD5	PerCP-Cy5.5	BD Biosciences	341089	L17F12	
Intranuclear staining with the True-Nuclear staining buffer kit					
True-Nuclear staining buffer kit	N/A	BioLegend	424401	N/A	
PU.1	Alexa Fluor 647	BioLegend	658004	7C6B05	
Mouse IgG1, κ isotype control (for PU.1)	Alexa Fluor 647	BioLegend	400136	MOPC-21	
GATA-2	FITC	R&D Systems	IC2046F	N/A	
Goat IgG isotype control (for GATA-2)	FITC	R&D Systems	IC108F	N/A	
GATA-1	PE	Cell Signaling Technologies	13353S	D52H6	
NF-kB p65	PE	Cell Signaling Technologies	9609S	D14E12	
Rabbit IgG isotype control (for GATA-1 and NF-κB p65)	PE	Cell Signaling Technologies	5742S	DA1E	

Table S2. List of reagents used. Related to Figures 1-5.

Transparent Methods

Experimental model and subject details

Human subjects

These studies are restricted to untreated CLL patients to eliminate confounding factors introduced by treatment. Fresh BM and/or blood samples were obtained from consenting CLL patients (Mayo Clinic IRB 1827-00, Table S1) and BM from age-matched controls either undergoing hip replacement surgery or recruited (Mayo Clinic IRBs 1062-00 and 16-006204) who signed informed consent per the Declaration of Helsinki and Mayo Clinic guidelines. BM samples were subjected to mature erythrocyte depletion by ACK lysis then used immediately. CLL blood samples underwent Ficoll separation immediately before use.

Cell lines

The murine stromal cell line M2-10B4 was obtained from ATCC and maintained in RPMI 1640 (Gibco) media supplemented with 10% fetal bovine serum (FBS, Mediatech), 1% penicillin/streptomycin (Gibco), and 1% L-glutamine (Gibco). The M2-10B4 cells were cultured in an incubator at 37^{o}C and 5% CO_2.

Method details

Flow cytometry

Following isolation, cells were Fc blocked (Miltenyi Biotec, San Diego, CA, USA). Surface staining with monoclonal antibodies and fixable viability dye was performed on ice in 1X PBS for 30 minutes. Following washing, the cells were fixed and permeabilized for 60 minutes according to manufacturer's directions (BioLegend, San Diego, CA, USA) to allow for intranuclear staining. Cells were then stained for 30 minutes at room temperature with monoclonal antibodies against nuclear targets or appropriate isotype controls. Following staining, cells were washed and suspended in 1% paraformaldehyde (Electron Microscopy Sciences, Hatfield, PA, USA) for acquisition. When cell surface staining only was performed, cells were washed twice following staining and fixed with 1% paraformaldehyde for acquisition. Flow cytometry data was collected on a FACS-Canto (Becton Dickinson, Franklin Lakes, NJ, USA) that is standardized daily to allow for direct comparisons of mean fluorescent intensity (MFI) across separate experiments(Manso et al., 2019; Perfetto et al., 2006; Perfetto et al., 2012).

Flow cytometry analysis

For analysis of PU.1, GATA-2, and NF-κB p65 relative protein levels, the MFI of the stained sample was subtracted against the appropriate isotype control as expression is unimodal (Figure 1D and Figure S1). The isotype-subtracted MFI is the value used in the figures. GATA-1 staining is bi-modal (Figure 1D and Figure S1). Therefore, relative protein levels of GATA-1 was determined by first gating on GATA-1 positive cells (determined by the isotype control), then calculating the MFI of GATA-1 among only the cells that are GATA-1^{+}. This process results in no isotype control staining in the GATA-1 histogram analysis by virtue of the initial GATA-1^{+} determination. Flow cytometry analysis was performed with FlowJo 10.5.3 (Becton Dickinson).

In vitro cell cultures

CD34^{+} cells from freshly processed control BM were isolated by positive magnetic bead selection (Miltenyi Biotec). CLL cells were plated at 1.0x10^{6} cells per well with 1.0x10^{5} CD34^{+} cells (10:1 ratio) in a 96 well round-bottom plate. The CLL:CD34^{+} co-cultures were incubated undisturbed for 24 hours at 37^{o}C 5%CO_2 in serum-free media (CellGenix, Portsmouth, NH, USA) supplemented with human recombinant stem-cell factor (10ng/mL), IL-6 (10ng/mL), IL-3 (1ng/mL), and erythropoietin (1ng/mL) (all from PeproTech, Rocky Hill, NJ, USA). Transwell (Corning, Corning, NY, USA) assays utilized a 1.0μm insert. CLL cells were plated in the Transwell with CD34^{+} cells in the lower chamber. Where indicated, 0.8μg of anti-TNFα antibody (R&D Systems, Minneapolis, MN, USA) was added to the cultures (in the lower chamber for Transwell experiments) at assay initiation. Recombinant human TNFα (R&D Systems) or IL-10 (BioLegend), when utilized, was added at 25ng/mL(Asano et al., 1999; Grigorakaki et al., 2011; Xiao et al., 2002) . In all cases, cells were stained for flow cytometry as outlined above to allow for detection of surface and intranuclear proteins.

Uniform manifold approximation and projection (UMAP)
The R program (version 3.6.1)(R Core Team, 2019) and the cytofkit2 package (Jinmiao Chen's Lab, version 2.0.1)(Becher et al., 2014; Chen et al., 2016; Wong et al., 2015) were used to generate UMAP(Leland McInnes, 2018) data and graphics plots from *ex vivo* and *in vitro* flow cytometry data. The single/live/Lin^- $CD34^{hi}CD38^-$ and $CD34^+CD38^+$ populations from each individual *ex vivo* sample was concatenated in FlowJo and exported whereas each *in vitro* flow cytometry data file was gated and exported on single/live/Lin^-/$CD34^+$ cells. The *ex vivo* data was imported into cytofkit2 with the parameters outlined in Figure S3A. Due to increased numbers of *in vitro* conditions/samples, additional data preprocessing was performed (Figure S3B). Some UMAP plots underwent additional graphical modifications with the ggplot2 package to allow for color selection and identical axis scaling across plots(Wickham, 2016).

Long-term culture initiating cell (LTC-IC) assay
Fresh BM $CD34^+$ cells from controls and CLL patients were isolated as above and plated across 12 or 36 replicates in LTC-IC medium (H5100 MyeloCult with 10^{-6}M hydrocortisone, StemCell Technologies, Vancouver, Canada). Cells were plated at limiting dilution (1000, 100, 50, 25, 10, 5, and 1 cell(s) per well) on irradiated feeder M2-10B4 stromal cells (12,500 cells per well) in 96 well flat-bottom plates. The cultures were maintained for five weeks at 37°C 5%CO_2 with weekly half-media exchange and scoring for the presence or absence of one or more colonies per well. In experiments containing TNFα, a limited cell dilution range was utilized (1000, 100, 50, and 10) with 12 replicates per dilution. Fresh media with the indicated concentration of TNFα was added weekly to the cultures to mimic *in vivo* chronic exposure.

Limiting dilution analysis (LDA)
Results from the LTC-IC assays containing control or CLL $CD34^+$ cells were analyzed by LDA (http://bioinf.wehi.edu.au/software/elda/)(Hu and Smyth, 2009). The confidence interval was set at 0.95, with options for testing inequality in frequency between multiple groups and adequacy of the single-hit model selected as analysis parameters.

Colony forming unit (CFU) assays
Following isolation of $CD34^+$ cells from freshly processed control BM, CFU assays were performed by plating triplicates of 500 $CD34^+$ cells in semisolid MethoCult H4435 media (StemCell Technologies). This media formulation allows for differentiation and enumeration of CFU-granulocyte, monocyte (CFU-GM), CFU-granulocyte, erythrocyte, monocyte, megakaryocyte (CFU-GEMM), and CFU-erythroid (CFU-E) colonies by morphology. When utilized, recombinant human TNFα was added at 25 ng/mL(Asano et al., 1999; Grigorakaki et al., 2011; Xiao et al., 2002). Neutralization of TNFα was achieved by addition of 0.8 μg of an anti-TNFα antibody (R&D Systems). The CFU cultures were incubated at 37°C 5% CO_2 for 11-12 days then manually scored, counted, and averaged across triplicates.

Quantification and statistical analysis
Statistical tests are indicated in figure legends and performed using GraphPad Prism version 8.1.2 (GraphPad Software, San Diego, CA, USA). For all tests, **P*<0.05, ***P*<0.01, ****P*<0.001, *****P*<0.0001, and "ns" indicates non-statistical significance. Note that, as some *ex vivo* and *in vitro* conditions had no detectable GATA-1, some paired t-tests are missing data for one or multiple conditions. When statistical analysis was performed, only values with data in each column were used for statistical comparison, as is standard practice. A power calculation was not performed owing to limited sample availability. Bar graphs of summary statistics indicate the mean ± standard error of the mean (SEM). The number of individual experiments and samples are outlined in the figure legends.

Supplemental references

Asano, Y., Shibata, S., Kobayashi, S., Okamura, S., and Niho, Y. (1999). Effect of interleukin 10 on the hematopoietic progenitor cells from patients with aplastic anemia. Stem Cells *17*, 147-151.

Becher, B., Schlitzer, A., Chen, J., Mair, F., Sumatoh, H.R., Teng, K.W., Low, D., Ruedl, C., Riccardi-Castagnoli, P., Poidinger, M.*, et al.* (2014). High-dimensional analysis of the murine myeloid cell system. Nat Immunol *15*, 1181-1189.

Chen, H., Lau, M.C., Wong, M.T., Newell, E.W., Poidinger, M., and Chen, J. (2016). Cytofkit: A Bioconductor Package for an Integrated Mass Cytometry Data Analysis Pipeline. PLoS Comput Biol *12*, e1005112.

Grigorakaki, C., Morceau, F., Chateauvieux, S., Dicato, M., and Diederich, M. (2011). Tumor necrosis factor alpha-mediated inhibition of erythropoiesis involves GATA-1/GATA-2 balance impairment and PU.1 over-expression. Biochem Pharmacol *82*, 156-166.

Hu, Y., and Smyth, G.K. (2009). ELDA: extreme limiting dilution analysis for comparing depleted and enriched populations in stem cell and other assays. J Immunol Methods *347*, 70-78.

Leland McInnes, J.H. (2018). UMAP: Uniform Manifold Approximation and Projection for Dimension Reduction. Preprint at https://arxivorg/abs/180203426.

Manso, B.A., Zhang, H., Mikkelson, M.G., Gwin, K.A., Secreto, C.R., Ding, W., Parikh, S.A., Kay, N.E., and Medina, K.L. (2019). Bone marrow hematopoietic dysfunction in untreated chronic lymphocytic leukemia patients. Leukemia *33*, 638-652.

Perfetto, S.P., Ambrozak, D., Nguyen, R., Chattopadhyay, P., and Roederer, M. (2006). Quality assurance for polychromatic flow cytometry. Nat Protoc *1*, 1522-1530.

Perfetto, S.P., Ambrozak, D., Nguyen, R., Chattopadhyay, P.K., and Roederer, M. (2012). Quality assurance for polychromatic flow cytometry using a suite of calibration beads. Nat Protoc *7*, 2067-2079.

R Core Team (2019). R: A language and environment for statistical computing (Vienna, Austria: R Foundation for Statistical Computing).

Wickham, H. (2016). ggplot2: Elegant Graphics for Data Analysis. Springer-Verlag New York.

Wong, M.T., Chen, J., Narayanan, S., Lin, W., Anicete, R., Kiaang, H.T., De Lafaille, M.A., Poidinger, M., and Newell, E.W. (2015). Mapping the Diversity of Follicular Helper T Cells in Human Blood and Tonsils Using High-Dimensional Mass Cytometry Analysis. Cell Rep *11*, 1822-1833.

Xiao, W., Koizumi, K., Nishio, M., Endo, T., Osawa, M., Fujimoto, K., Sato, I., Sakai, T., Koike, T., and Sawada, K. (2002). Tumor necrosis factor-alpha inhibits generation of glycophorin A+ cells by CD34+ cells. Exp Hematol *30*, 1238-1247.